DRF

RESEARCH REPORT

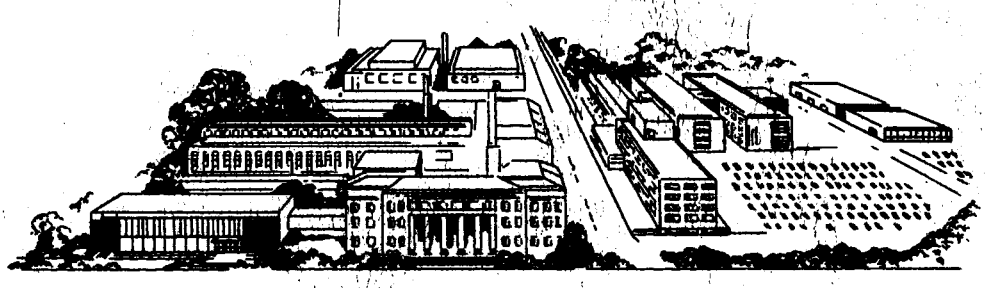

BATTELLE

MEMORIAL INSTITUTE

BATTELLE FIELDS OF RESEARCH

Aeronautics—Astronautics
Agricultural Chemistry
Agricultural Economics
Alloy Development
Applied Mathematics
Area Economics
Biochemistry
Biophysics—Bionics
Catalysis—Surface Chemistry
Ceramics
Chemical Engineering
Chemical Processes
Communications Science
Computer Technology
Corrosion Technology
Earth — Atmospheric Sciences
Electrochemistry
Electronics
Energy Conversion
Engineering—Structural Materials
Environmental Systems
Extractive Metallurgy
Extreme-Temperature Technology
Ferrous Metallurgy
Food Technology
Foundry Practice
Fuels—Combustion
Glass Technology
Graphic Arts Technology
Immunology—Cancer Studies
Industrial Economics
Industrial Physics
Information Research
Inorganic Chemistry
Instrumentation
Light Alloys—Rare Metals
Lubricant Technology
Materials Separation—Concentration
Mechanical Engineering
Metal Fabrication Engineering
Metal Finishing
Metallurgical Processes
Microbiology
Microscopy—Mineralogy
Nondestructive Evaluation Technology
Nonferrous Metallurgy
Nucleonics
Organic Chemistry
Organic Coatings
Packaging Research
Particle Dynamics
Petrochemicals
Petroleum Engineering
Pharmaceutical Chemistry
Physical Chemistry
Product Development
Production Engineering
Psychological Sciences
Pulp—Paper Technology
Radioisotopes—Radiation
Reactor Technology
Refractories
Reliability Engineering
Rubber—Plastics
Semiconductors—Solid-State Devices
Sound — Vibration
Systems Engineering
Textiles—Fibers
Theoretical—Applied Mechanics
Thermodynamics
Transportation
Welding—Metals-Joining Technology
Wood—Forest Products

MIDPOINT REPORT
Contract No. NAS3-2797

on

ALPHA-CELL DIRECT-CONVERSION GENERATOR

to

LEWIS RESEARCH CENTER
NATIONAL AERONAUTICS AND
SPACE ADMINISTRATION

August 19, 1964

by

A. M. Plummer, W. J. Gallagher,
R. G. Matthews, and J. N. Anno

Lewis Research Center Report Number CR-54162

BATTELLE MEMORIAL INSTITUTE
505 King Avenue
Columbus, Ohio 43201

TABLE OF CONTENTS

TABLE OF CONTENTS
(Continued)

ALPHA-CELL DIRECT-CONVERSION GENERATOR

by

A. M. Plummer, W. J. Gallagher, R. G. Matthews, and J. N. Anno

INTRODUCTION

Under contract with the Lewis Research Center of the National Aeronautics and Space Administration, Battelle is currently studying a generator which converts alpha-particle energy directly into electricity. The conversion is accomplished by causing the high-energy alpha particles to do work against an electric field. This concept is referred to as the alpha electric cell, or simply the alpha cell. A source material such as polonium-210, or other high-energy alpha emitter, is distributed in a thin layer over a surface which will be called the cathode. The emitting surface is capable of charging a collecting electrode, which will be called the anode. In time a retarding electric field is established, and the positively charged alpha particles do work against this field, i.e., their kinetic energy is transformed to available electrical energy. The alpha cell is basically a high-voltage (megavolt range), low-current device.

The power range for a generator based on this direct-conversion concept is not yet firmly established. However, it appears at present that generators with useful outputs of 10 to 100 watts may be achieved. The applications for such a generator are likewise unspecified at this early stage in development. Applications as primary or auxiliary space power for satellites are visualized, but other applications might prove to be of greater interest. For example, the alpha cell could serve as the high-voltage source for an electrostatic propulsion unit using heavy particles; it could also serve as the high-voltage source for antennae for satellite communications. As the operating characteristics and practicality of the concept become better known, the applications should become more evident.

Battelle-sponsored experiments performed in late 1962 showed that the principles of operation of the device were sound in the relatively low-voltage range obtained at that time (approximately 50,000 volts).* However, for efficient operation the device must operate in the range near 1 megavolt. The objective of the current program is to extend the voltage capability of the alpha cell to this higher range and to determine the characteristics of the cell under this condition. This report presents the results of the first-half of an 8-month study.

Since the ideas behind the alpha-cell concept may not be known by some of the readers of this report, the report contains a review of the principles of operation and a summary of the results of previous studies at Battelle, along with a summary of research under the current contract. This information embodies essentially everything we know to date about the concept, with the exception of knowledge that will be gained from studies now under way on high-voltage conversion concepts, which are just briefly summarized. It is planned that the second 4-month period of research will concentrate on analysis of the experimental results and on certain other analyses pertinent to cell behavior.

*Publications summarizing the results of the Battelle-sponsored experiments are listed as Bibliography on page 65.

As with any concept, the alpha cell presents problems. Principal among these is sustaining the high-voltage electricity produced and converting it to lower voltages. Whether or not these problems will be insurmountable must await results of further studies. At present, we have reason to be optimistic as will be seen from the results of the experiments. Comments from interested persons on this concept and on the results presented in this report are encouraged.

The Battelle team participating in this study is listed as the authors of this report. The contract for this work is being administered at Lewis Research Center by Mr. John E. Dilley, Contracting Officer, with Mr. Ernest Koutnik, Nuclear Power Technology Branch, as Project Manager. Mr. William R. Mickelsen, Chief, Electrostatic Propulsion Branch, and Mr. Charles A. Low, Jr., are acting as technical advisors for this project, and both are members of the staff of the Electromagnetic Propulsion Division at the NASA, Lewis Research Center.

THEORY OF ALPHA-CELL OPERATION

This section of the report presents the theory of alpha-cell operation in its present state of development. In this discussion, the currents, efficiencies, etc., relate to a single isolated cell. Further, the change in efficiency due to the high-voltage conversion technique is not considered here since this area is undergoing preliminary study.

FUNDAMENTAL PRINCIPLES OF OPERATION OF THE ALPHA CELL

The alpha particle, with mass of 4.003 amu, is essentially a helium atom with the two electrons removed. Certain radioisotopes decay by emission of an alpha particle, the half-life of the decay varying widely with the isotope. The half-life ranges from 3×10^{-7} sec for polonium-212 (ThC') to 1.4×10^{10} years for thorium-232. The alpha particles thus emitted are monoenergetic, with energies for isotopes of interest typically in the range of 5 to 6 Mev. At birth each alpha particle has a charge of +2. A brief reflection on this fact points out the underlying principle of the alpha cell process: in the phenomenon of alpha decay we have electricity in its most elementary form – charged particles in motion.

The more conventional methods of using radiosotope energy do not make use of the alpha-particle kinetic energy and positive charge in a direct manner. Rather, the alpha particles dissipate their energy and charge in a thick fuel material, producing heat. The heat generated in the fuel is typically used to raise the temperature of a thermionic or thermoelectric material which, in turn, produces electricity.

However, if the isotope is distributed in a sufficiently thin layer rather than in a thick fuel region, so that an appreciable fraction of all the alpha particles produced in the layer can escape from the surface with much of their initial energy and charge intact, these particles can be collected on an insulated electrode. The first few alphas reaching the electrode will deposit their charge and dissipate their kinetic energy as heat. However, after a number of alphas have been collected, the insulated electrode, by virtue of its surplus of positive charge, will attain a high voltage with respect to the emitter layer. Subsequent alpha particles will "do work" against this electric field: they will arrive at the electrode with their initial kinetic energy exhausted but will deposit their charge. The space between the electrodes is evacuated to prevent energy loss by ionization of intervening gas and to permit high voltage buildup by serving as an electrical insulator. The voltage characteristic of this process is (E_o/Z_o), the ratio of the initial kinetic energy of the alpha particle in electron volts divided by its charge magnitude. This follows from the definition of the electron volt as the work done per unit charge when the unit charge is moved through a potential difference of one volt. Since E_o is typically of the order of 5-million electron volts and Z_o is +2, the characteristic voltage of the process is several megavolts.

In effect, the arrangement discussed above is analogous to a capacitor, as shown in Figure 1, with the alpha particles doing the charging. The charge separation caused by the energetic alpha particles driving their way to the insulated electrode, the

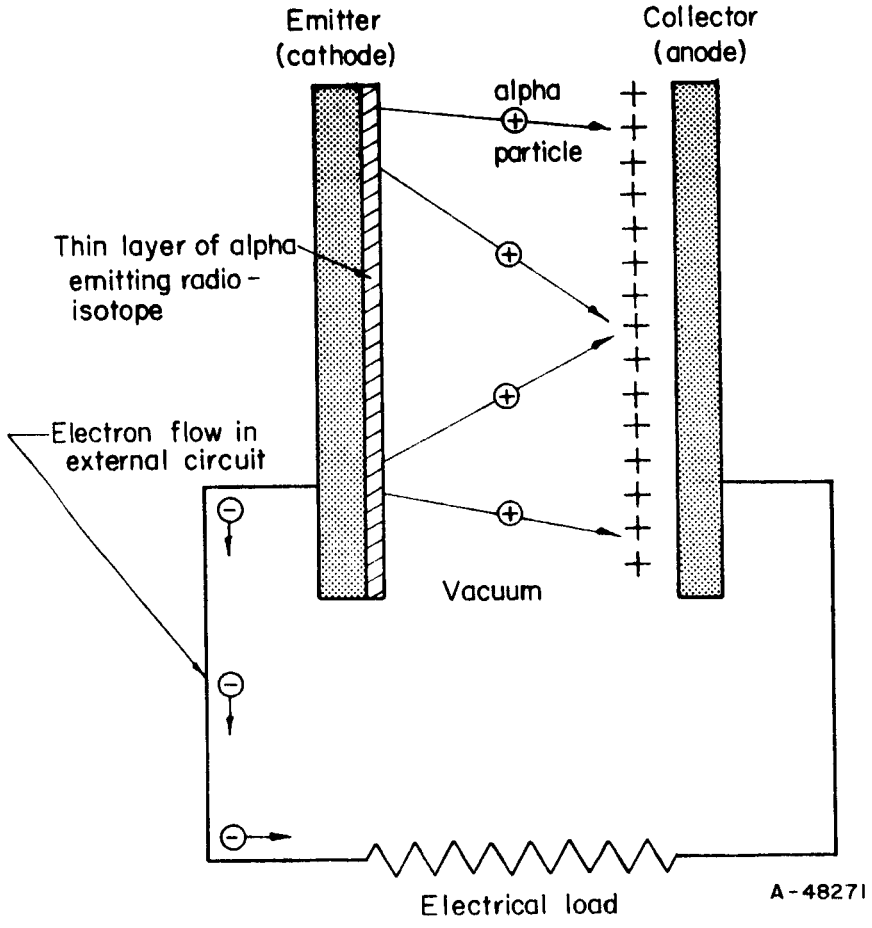

FIGURE 1. THE PRINCIPLE OF THE ALPHA CELL'S OPERATION

collector, is neutralized by a flow of the electrons which were left behind through an external circuit. This electron flow through an external circuit is a source of direct electricity produced without the use of a heat cycle. The high-voltage d-c electricity thus produced can be used directly, reduced to a lower voltage or inverted to a-c electricity. The direct conversion occurs in the use of the alpha-particle kinetic energy to effect a charge separation across a high potential difference.

The discovery that charged-particle emission can build up a voltage on a properly insulated electrode may be traced to work by Mosely in 1913.[1]* The direct application of this idea for a high-voltage generator has been considered by others during the past several decades, for example, the work of Linder and Christian at RCA.[2] However, a critical problem exists in reducing the concept to practice. Along with the positively charged alpha particles come secondary electrons which have an opposing charge. Measurements indicate that approximately 10 secondary electrons are released from the surface with each alpha particle.[3] Although these secondary electrons have very low energy (approximately 97 per cent have energy less than 100 ev), they are produced in such abundance that their total negative charge more than offsets the positive-charge buildup. Thus, a low-energy net negative charge, rather than the desired positive high-energy charge, is emitted from the cathode.

A properly designed control grid placed close to the cathode can be used to overcome this difficulty. A negative potential applied to the grid will repel the secondary electrons to the cathode. A simple configuration which illustrates the concept is shown in Figure 2. A cylindrical electrode, the emitter or cathode, can be a tube or rod coated with a layer of alpha emitter several microns thick. This thickness is required since the range of alpha particles in metals is of the order of 10 microns. Surrounding the cathode in this example is a "squirrel-cage" grid at negative voltage with respect to the cathode. The grid is composed of small-diameter wires and is sufficiently open to permit the alpha particles to reach the collector, or anode, while at the same time preventing the secondary electrons from escaping. Because the electrons have very low energy, only a few hundred volts' bias on the grid will suppress them. To hold back the electrons when the anode is at several million volts requires an increase in voltage to the kilovolt range. The grid can be designed to be almost completely open; typically 90 per cent or more of the total grid area is not blocked by grid wires.

From the previous discussion it is apparent that the grid is the key to the successful operation of the alpha cell. As will be discussed in a later section of the report, its design has a considerable bearing on the efficiency of the operation and may acquire added significance in the conversion of the high voltage d-c electricity to lower voltage a-c electricity. One can also conceive of suppressing the secondary electrons with a magnetic field, but for reasons which will be discussed later, under existing technology the use of a grid appears to have a significant advantage.

CONVERSION EFFICIENCY OF IDEAL CELLS

The efficiency of conversion of alpha-particle kinetic energy into electrical energy is dictated principally by the geometry of the alpha cell. In this section, the conversion will be derived for ideal cells, those which contain a transparent yet completely

*References are listed on page 64.

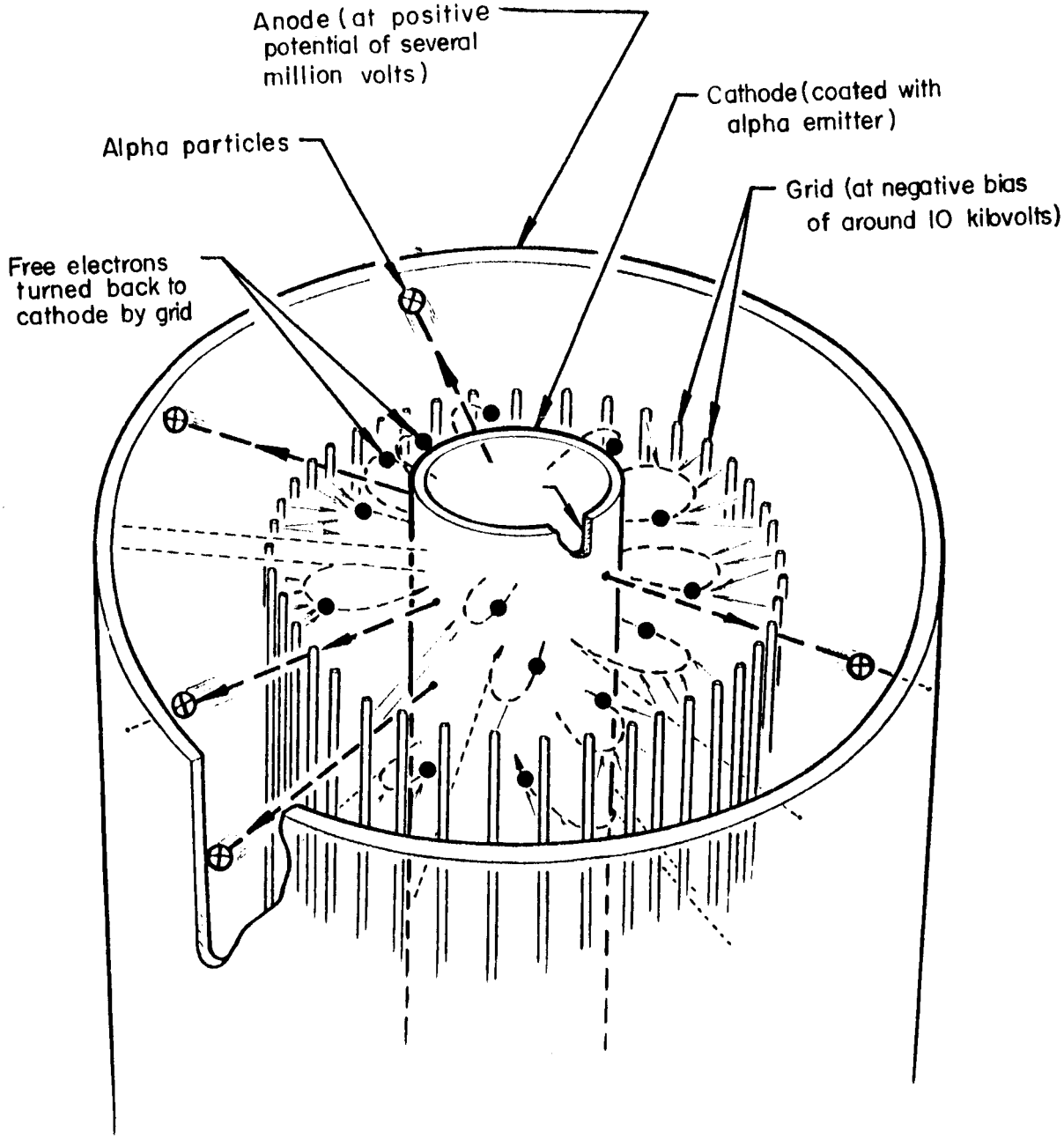

FIGURE 2. USE OF A GRID TO REPEL SECONDARY ELECTRONS (COAXIAL-CYLINDER GEOMETRY)

effective grid. The effects of geometry on conversion efficiency can best be illustrated by discussing the more common geometries: parallel planes, coaxial cylinders, and concentric spheres.

Efficiency for Common Geometries

For the initial calculation of efficiencies, it will be assumed that the total cell efficiency is purely a geometrical one. The thickness of isotope of the emitter will be assumed sufficiently thin that no energy losses are incurred in the alphas escaping from the fuel. By the same token, the alpha particles will be assumed to be mono-energetic. (It will later be shown that one of the effects of a finite fuel layer is to spread the energy distribution of the alpha particles.)

Concentric Spheres

The most efficient but perhaps least practical geometry for the alpha cell is that of a concentric, spherical emitter and collector. In the limit of large collector diameter compared with emitter diameter, this case is that of a point source emitter surrounded by a spherical collector. All alpha particles are emitted radially and hence normal to the collector surface. As can easily be seen, the conversion efficiency P in this case is

$$P = \frac{1}{2}\frac{VZ_o}{E_o} = \beta/2 \quad , \tag{1}$$

where $\beta = \frac{VZ_o}{E_o}$ is a dimensionless voltage parameter ranging from 0 to 1. The factor of 1/2 in this relation arises from the fact that for a thick fuel substrate only 1/2 of the alpha particles are directed radially outward; the other half embed in the cathode structure. Thus, for concentric spheres the efficiency increases linearly with anode voltage, reaching 50 per cent for the maximum possible voltage of (E_o/Z_o).

Coaxial Cylinders

In a coaxial-cylinder geometry with the cathode diameter small compared with the anode diameter (in the limit, a line source cathode coaxial with a cylindrical anode), the efficiency can be calculated as follows. If n_o represents the total number of alpha particles produced per unit time, then half of the particles, $n_o/2$ will be emitted with an outward radial component. With the anode at some voltage V with respect to the cathode, some of these particles will have insufficient velocity component perpendicular to the anode to reach it. The initial particle velocity is $v_o = \sqrt{\frac{2E_o}{m}}$ where m is the alpha-particle mass. The radial component of the initial velocity is $v_o \cos\theta$, where θ is the angle which the path of the particle makes with the normal to the emitting surface. For the alpha particle to overcome the electric field to arrive at the anode, it is necessary that

$$\frac{m(v_o \cos\theta)^2}{2} \geq VZ_o \quad ,$$

or, hence, that

$$E_o \cos^2\theta \geq VZ_o \quad . \tag{2}$$

The maximum angle, θ_{max}, at which an emitted particle will just reach the anode is seen from Equation (2) to be given from the relation

$$\cos \theta_{max} = \sqrt{\frac{VZ_o}{E_o}} = \sqrt{\beta} \ . \tag{3}$$

Particles emitted at angles less than θ_{max} will reach the anode; those emitted at angles greater than θ_{max} will not.

In the coaxial-cylinder configuration, the number which reach the anode for isotropic emission is*

$$n = \frac{n_o}{2} \sin \theta_{max} = \frac{n_o}{2} \sqrt{1 - \frac{VZ_o}{E_o}} \ , \tag{4}$$

and the conversion efficiency is

$$P = \frac{n}{n_o} \frac{VZ_o}{E_o} = \frac{1}{2} \frac{VZ_o}{E_o} \sqrt{1 - \frac{VZ_o}{E_o}} = \frac{\beta}{2} \sqrt{1-\beta} \ . \tag{5}$$

This equation shows a maximum efficiency of about 19 per cent for $\beta = 2/3$. (See Figure 3). Using as characteristic values $Z_o = 2$ charges and $E_o = 5$ Mev, the voltage at maximum efficiency is 1.7 megavolts.

Parallel Planes

For the case of parallel planes infinite in extent, integration over the particles emitted within the angular range $0 \leq \theta \leq \theta_{max}$ gives directly

$$n = \frac{n_o}{2} (1 - \cos \theta_{max}) = \frac{n_o}{2} \left(1 - \sqrt{\frac{VZ_o}{E_o}} \right) , \tag{6}$$

and the conversion efficiency is

$$P = \frac{n}{n_o} \frac{VZ_o}{E_o} = \frac{\beta}{2} \left(1 - \sqrt{\beta} \right) \ . \tag{7}$$

For this configuration, maximum conversion efficiency is 7.4 per cent for $\beta = 4/9$ (1.1 megavolts when using the values of $Z_o = 2$ and $E_o = 5$ Mev as in the previous example).

Figure 3 is a graphical representation of the efficiencies for the three common geometries considered above. This comparison illustrates the gain in efficiency to be made in progression from parallel-plane to spherical geometry. It also shows that, for the cases of coaxial cylinders or parallel planes, the efficiency curve has a rather broad maximum. This means that in these geometries, precise control of anode voltage is not necessary to maintain efficiency near the optimum value.

Table 1 summarizes the maximum conversion efficiencies attainable with three common geometries. In the simplest cases previously calculated, the fuel would be deposited in a thin layer on a thick substrate so that only half of the alpha particles could escape from the surface. In more advanced designs, it is possible to visualize two-sided emission geometries (fuel deposited on a screen-like substrate, fuel in the form of thin wires or gauze, etc.).

*The required integration is most readily performed by first considering the number of particles missing the anode, i.e., integrating from θ_{max} to $\pi/2$.

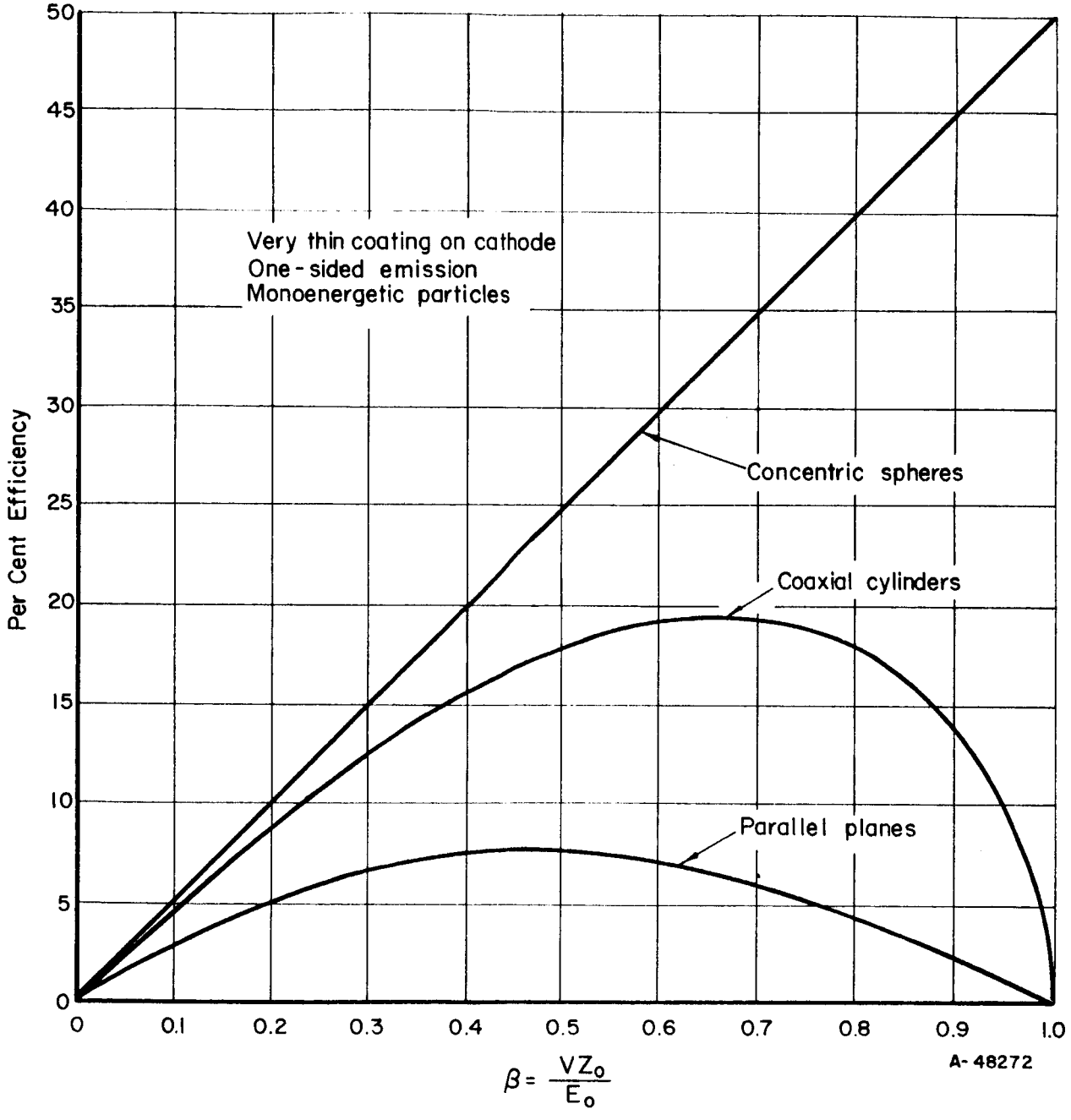

FIGURE 3. EFFICIENCY VERSUS VOLTAGE FOR THREE COMMON GEOMETRIES

TABLE 1. MAXIMUM CONVERSION EFFICIENCIES FOR THREE COMMON GEOMETRIES

Geometry	Maximum Theoretical Efficiency	
	One-Sided Emission	Two-Sided Emission
Parallel planes	7.4	14.8
Coaxial cylinders	19.2	38.4
Concentric spheres	50.0	100.0

Similar efficiency calculations can be made for these geometries in which the cathode diameter is a significant fraction of anode diameter. As would be expected, these cases are intermediate between the ones presented here. A fact which is perhaps not obvious is that by selective choice of an "uncommon" finite geometry, efficiencies greater than that of the infinite coaxial-cylinder geometry can possibly be obtained in quasicylindrical geometry. The choice of geometry is not simply one between cylindrical or spherical, but of any compromise of the two.

CELL CURRENTS IN GRIDDED DEVICES

The presence of a grid modifies the charging current to the collector due to several effects. Cell currents in a gridded device are discussed below under various conditions.

Currents With Anode at Zero Voltage

The expressions for the currents in a gridded device can be derived from the following definitions.

I_o = current carried from cathode by positively charged alpha particles

f = fraction of alpha particles emerging from the cathode which strike the grid wires

x = fraction of secondary electrons produced at the grid which escape the grid-cathode assembly,

η_g = charge ratio, the magnitude of the ratio of the secondary electrons produced at the grid to the charge of alpha particles striking the grid.

It is assumed that the grid is at large negative bias, the condition required for cell operation. Considering first the grid current, the fraction f of the alpha particles striking the grid carry current of positive charges of ($f I_o$) to the grid. These alpha particles striking the grid produce secondary electrons, so that a secondary-electron current of ($f \eta_g I_o$) is produced at the grid. Since the grid is at a large negative bias, all of these secondaries escape from the grid. The total current from the grid is the sum of the two components:

$$I_g = I_{grid} = -(f\, I_o) - (f\, \eta_g I_o) = -\, f\, (1 + \eta_g)\, I_o \qquad (8)$$

This current is supplied by the grid power supply, but since it is supplied at a voltage much less than the anode voltage, the power expenditure is negligible. The minus sign is assigned to this current according to the convention that a flow of positive charges from the cathode is a positive current. The cathode current also consists of two components. A current I_o of alpha particles leaves the cathode, but a fraction $(1 - x)$ of the secondary electrons produced by the few alphas which strike the grid returns to the cathode. The cathode current is then

$$I_{co} = I_{cathode} = I_o + (1 - x)\, (f\, \eta_g\, I_o) = [1 + (1 - x)\, f\, \eta_g] I_o \qquad (9)$$

The net current from the grid-cathode assembly is the algebraic sum of the grid and cathode currents and represents the current available to charge the anode.

$$I_c = I_{net} = [(1 - f) - x\, f\, \eta_g]\, I_o = [1 - f\, (1 + x\, \eta_g)]\, I_o \qquad (10)$$

It will be noted that this charging current is diminished from the original alpha-particle current I_o by two factors. First, due to the physical interception of some alpha particles by the grid, only $(1 - f)$ of the alpha particles escapes from the grid-cathode assembly. Second, a fraction x of the secondary electrons formed at the grid escapes to the anode and reduces the net flow of positive charge. Note that the loss in charging current is proportional to $f\, (1 + x\, \eta_g)$. It is apparent that the interception fraction at the grid, the f-factor, must be as small as possible to minimize losses in the charging current. How this bears on grid design will be discussed later.

Figure 4 shows how these currents would be expected to behave as a function of grid bias. Below about 100 volts on the grid, the energy distribution of the secondary electrons will affect the currents. At high negative grid bias, these currents should be independent of grid bias. From the previous analyses, as shown in Figure 4, the cathode current would be expected to be larger than the alpha-particle current by an amount $(1 - x)\, f\, \eta_g\, I_o$, which represents a flow of secondary electrons formed at the grid back to the cathode. Of course, it would be hoped that the grid current is small enough that a positive net current is obtained from the device, i.e., $I_{co} + I_g > 0$. It should be mentioned that these current relations are simplified to the extent that second-order effects have been neglected, such as the formation of secondary electrons by gamma radiation accompanying the alpha decays. However, for an alpha emitter such as polonium-210, these relations should be a good approximation to the actual currents.

Currents at Large Anode Voltage (Common Geometries)

As seen from the calculations of efficiency for the common geometries, the current to the collector generally decreases with increasing anode voltage (except for the concentric spherical case with point source anode) due to the repulsion of the alpha particles by the electric field. For an ideal grid (f-factor of zero), the behavior of the charging current with anode voltage in the three cases derived previously is

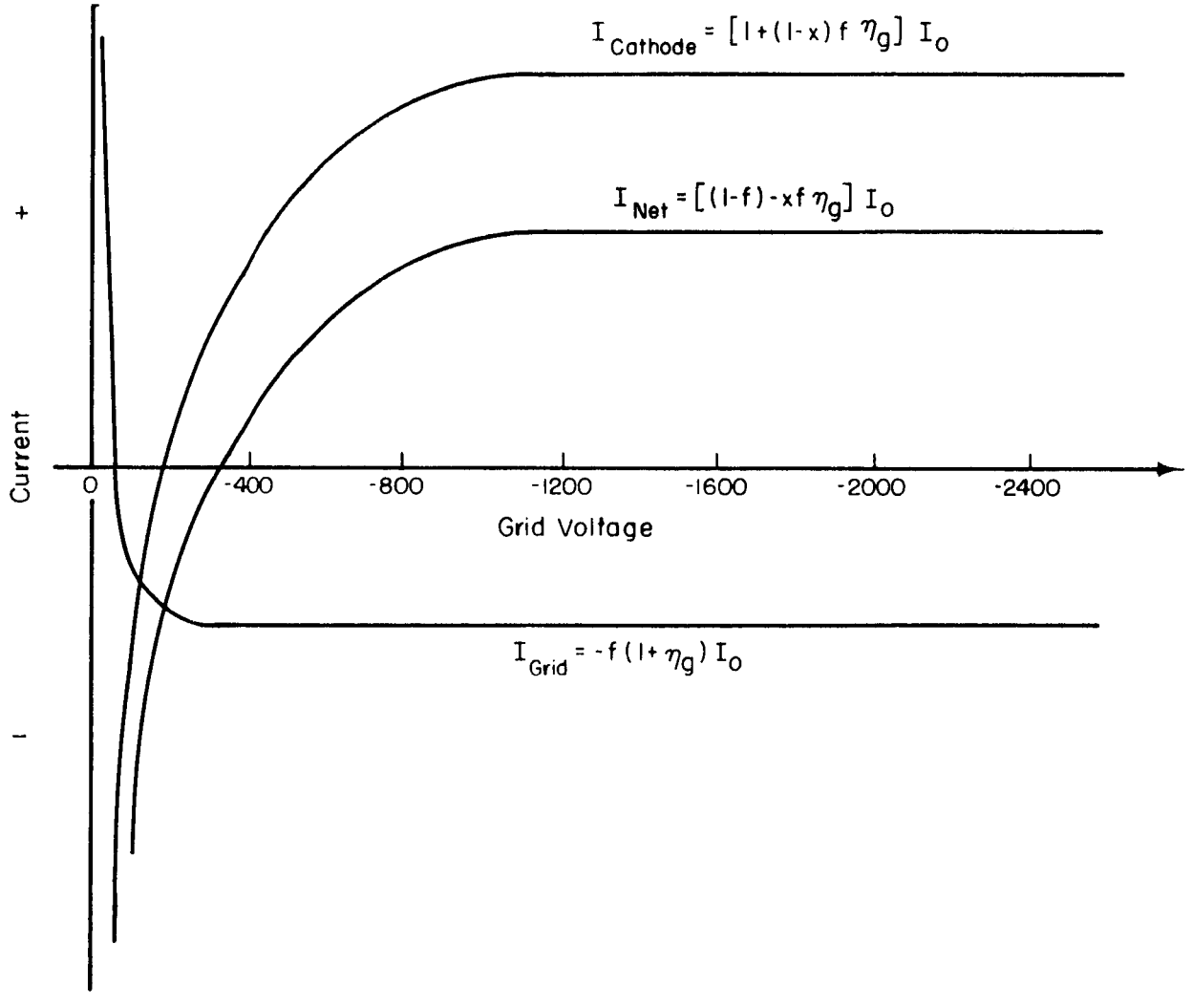

FIGURE 4. BEHAVIOR OF CURRENTS WITH GRID VOLTAGE FOR AN IDEAL ALPHA CELL (ZERO ANODE VOLTAGE)

$$I_c = I_o \qquad \text{(concentric spheres)} \qquad (11)$$

$$I_c = I_o \sqrt{1 - \frac{VZ_o}{E_o}} \qquad \text{(coaxial cylinders)} \qquad (12)$$

$$I_c = I_o \left(1 - \sqrt{\frac{VZ_o}{E_o}}\right) \text{(parallel planes)} \qquad (13)$$

The previous discussion considered the modification to the charging current at zero anode voltage due to a grid with finite f-factor, and the grid, cathode, and net currents were derived under these conditions. At large anode voltage another effect, apart from repulsion of the alphas by the field, also appears due to the grid. This effect is the striking of the grid by the "fall-back" particles, i.e., by those alpha particles which initially escape the grid-cathode assembly but do not have sufficient energy to reach the collector. The derivation and consequences of this effect will be briefly discussed. As might be expected, the analysis again emphasizes the importance of grid design, viz., of a low f-factor grid, and the importance of the geometry of the cell.

To illustrate the derivation of the expressions for the cell currents, coaxial-cylinder geometry will be used in the analysis. The extension to other geometries follows immediately. It is convenient to define the following terms, which are similar in definition to their counterparts used in the analysis of the cell currents at zero anode voltage. Let

f' = fraction of fall-back alpha particles which strike the grid on return toward the cathode.

η_g' = magnitude of the charge ratio of secondary electrons to fall-back particles which strike the grid. (This may differ from η_g due to angular variations in the striking particles.)

x' = fraction of the secondaries formed at the grid by the fall-back particles which escapes to the anode; $(1 - x')$ escapes to the cathode.

Then the grid current at large anode voltage is

$$I_g = \underbrace{-f(1 + \eta_g)I_o}_{\text{low-voltage current}} \underbrace{- f'(1 - f)\left[1 - \sqrt{1 - \frac{VZ_o}{E_o}}\right] I_o}_{\text{current to grid from fall-back particles which strike the grid on return to the cathode}}$$

$$\underbrace{- f'\eta_g'(1 - f)\left[1 - \sqrt{1 - \frac{VZ_o}{E_o}}\right] I_o}_{\text{secondary-electron current produced by the fall-back particles at the grid}}$$

$$= -f(1+\eta_g)\,I_o - f'(1+\eta_g')(1-f)\left[1-\sqrt{1-\frac{VZ_o}{E_o}}\right]I_o$$

$$= (I_g)_o\left\{1+\frac{f'(1-f)}{f}\frac{(1+\eta_g')}{(1+\eta_g)}\left[1-\sqrt{1-\frac{VZ_o}{E_o}}\right]\right\}. \qquad (14)$$

where $(I_g)_o$ is the grid current at zero anode voltage. Next, examining the cathode current,

$$I_{co} = \underbrace{[1+(1-x)f\eta_g]I_o}_{\text{low-voltage current}} - \underbrace{(1-f')(1-f)\left[1-\sqrt{1-\frac{VZ_o}{E_o}}\right]I_o}_{\text{charged-particle current returning to the cathode due to the fall-back particles which get past the grid}}$$

$$\underbrace{+(1-x')f'\eta_g'(1-f)\left[1-\sqrt{1-\frac{VZ_o}{E_o}}\right]I_o}_{\text{secondary-electron current flowing to cathode due to fall-back particles which strike the grid}}$$

$$= [1+(1-x)f\eta_g]I_o - [(1-f')-(1-x')f'\eta_g'](1-f)\left[1-\sqrt{1-\frac{VZ_o}{E_o}}\right]I_o$$

$$= (I_{co})_o\left\{1-\frac{[(1-f')-(1-x')f'\eta_g'](1-f)\left[1-\sqrt{1-\frac{VZ_o}{E_o}}\right]}{[1+(1-x)f\eta_g]}\right\}, \qquad (15)$$

where $(I_{co})_o$ is the cathode current at zero anode voltage.

The net current, which is the charging current available to charge the anode, is the algebraic sum of the grid and cathode currents and can be written as

$$I_c = I_{co} + I_g$$

$$= [1-f(1-x\eta_g)I_o - [1-f'(1-x'\eta_g')](1-f)\left[1-\sqrt{1-\frac{VZ_o}{E_o}}\right]I_o$$

$$= (I_c)_o\left\{1-\frac{[1-f'(1-x'\eta_g')](1-f)\left[1-\sqrt{1-\frac{VZ_o}{E_o}}\right]}{[1-f(1+x\eta_g)]}\right\}, \qquad (16)$$

where $(I_c)_o$ is the net current at zero anode voltage. This relation can be written in more compact form as

$$I_c = (I_c)_o \left\{ 1 - k \left[1 - \sqrt{1 - \frac{VZ_o}{E_o}} \right] \right\} , \tag{17}$$

where

$$k = \frac{[1 - f'(1 - x'\eta_g')]\,(1 - f)}{[1 - f(1 + x\eta_g)]} , \tag{18}$$

and $k \geq 1$ always. Note that for a perfectly transparent grid ($f' = f = 0$), we have

$$I_c = (I_c)_o \sqrt{1 - \frac{VZ_o}{E_o}} , \tag{19}$$

which is equivalent to Equation (12). It is seen from Equation (17) that the effect of the "fall-back" particles is to reduce the charging current to the anode. The smaller the value of k, the less the reduction.

Similar considerations to those above for the coaxial-cylinder geometry lead to a charging current for the parallel-plane case at large anode voltage of

$$I_c = (I_c)_o (1 - k\sqrt{\beta}) . \tag{20}$$

Note that in the ideal case of concentric spheres, where the cathode is small enough to appear as a point source to the collector, there are no fall-back particles, which further emphasizes the desirability of spherical geometry. Of course, when the emitted particles are not monoenergetic, a fall-back problem arises even in the spherical case.

The factors appearing in the expressions for the cell currents at large anode voltage should be independent of anode voltage, except perhaps the x and x′ factors. The fraction of secondary electrons formed at the grid which escape to the anode is sensitive to the configuration of the electric field in the vicinity of the grid wires.

CONVERSION EFFICIENCY OF GRIDDED DEVICES

The conversion efficiency of ideal alpha cells (completely transparent but completely effective grid) was discussed earlier. This section of the report analyzes briefly the effect of a grid with finite f-factor on conversion efficiency. As before, the discussion is presented in terms of the three common geometries with only a brief look at uncommon ones.

Common Geometries

Concentric Spheres

As shown previously, the concentric spherical geometry, with emitter diameter much smaller than collector diameter, is unique in that there is ideally no problem

with fall-back alpha particles. In this case, the only effects of the grid are the blockage of a small fraction of the alpha particles and a current loss due to secondary-electron production at the grid. The efficiency in this geometry for a gridded device is thus

$$P = C\beta \tag{21}$$

where $C = \frac{(I_c)_o}{2I_o}$ and $(I_c)_o$ is defined from Equation (10). As the grid approaches transparency, C approaches 1/2 and Equation (21) becomes identical with the efficiency expression developed for an ideal grid.

Coaxial Cylinders

In the coaxial-cylinder geometry with emitter diameter << collector diameter, the expression for efficiency in a gridded device becomes

$$P = C\beta\left[(1 - k) + k\sqrt{1 - \beta}\right] \tag{22}$$

compared with $P = 1/2\ \beta\sqrt{1 - \beta}$ for the ideal case. Expressed in this fashion, $C = \frac{(I_c)_o}{2I_o}$ accounts for the effects of grid blockage and k for the effects of the fall-back alphas. By differentiation of this expression, it can be seen that peak efficiency occurs at a voltage given by

$$\beta = \frac{2}{9}\left[(3 - q) - \sqrt{q(q + 3)}\right] \tag{23}$$

where $q = \left(\frac{k-1}{k}\right)^2$. Note that when k = 1 (transparent grid), $\beta = 2/3$ for peak efficiency, but as k increases from unity, the voltage at which maximum efficiency occurs decreases.

Parallel Planes

Similar analysis shows that for a parallel-plane geometry infinite in extent, for a gridded device

$$P = C\beta(1 - k\sqrt{\beta}) \ , \tag{24}$$

compared with the ideal efficiency of $P = 1/2\ \beta\ (1 - \sqrt{\beta})$. The effects of the grid are similar to those in the coaxial cylinder case.

The analyses clearly show that, except for the ideal concentric spherical geometry, it is extremely important to minimize the factor k in a device constructed in a geometry approximately one of the common geometries. The effect of a grid on efficiency is illustrated in Figure 5 for several values of k and for a coaxial-cylinder geometry. The values of k selected for this illustration correspond approximately to the following parameters:

k = 1: a transparent grid, $f' = f = 0$

k = 1.5: a "reasonable" grid, $f' = f = 0.1$

k = 5: a worst case, $f' = 1.0$, $f = 0.1$,

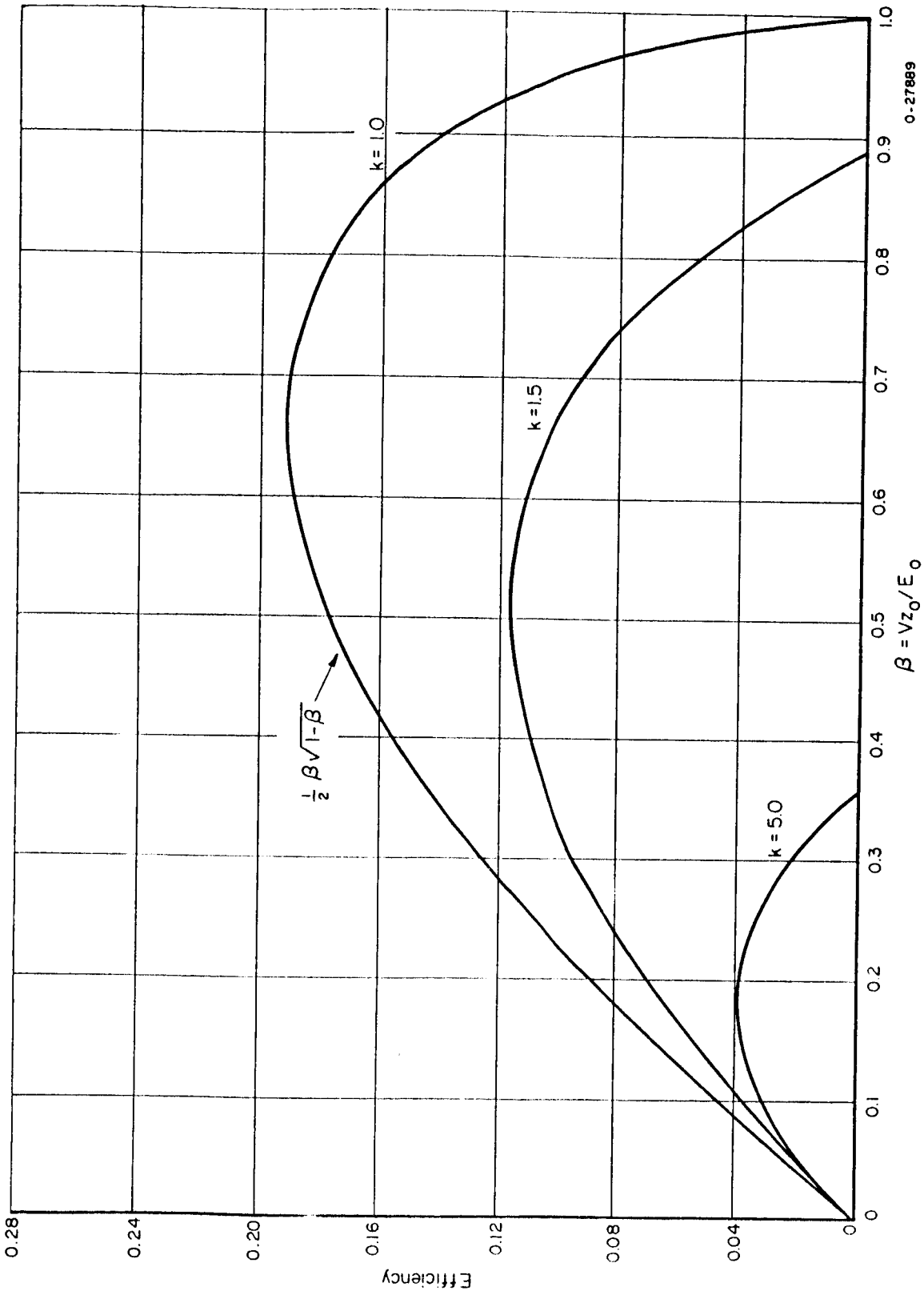

FIGURE 1. EFFICIENCY FOR COAXIAL CYLINDRICAL GEOMETRY
Thin film coating; one-sided emission

FIGURE 5. EFFICIENCY FOR COAXIAL CYLINDRICAL GEOMETRY WITH GRID

Thin-film coating; one-sided emission

where, for the sake of example, values of the other parameters have been selected as $x = 0.1$, $x' = 1.0$, $\eta_g = \eta_g' = 5$. It is seen from this graph that for a k value of only 1.5, the peak efficiency is reduced from 19 per cent in the ideal case to approximately 12 per cent. A large k reduces efficiency even more drastically.

Uncommon Geometries

Although each geometry must be considered separately, several general facts can be pointed out concerning the efficiency of gridded devices in the uncommon geometries. If complete electrostatic focusing of the alpha particles away from the grid is accomplished in a certain geometry, the fall-back problem with the alpha particles is completely removed. In this case the only effects of the grid are blockage of alpha particles and production of secondary electrons; i.e., $k = 1$ and the change in efficiency from an ideal device is contained in the factor $C = \frac{(I_c)_o}{2I_o}$. This savings provides further incentive to seek geometries in which at least partial electrostatic focusing can be accomplished.

GRID-DESIGN PRINCIPLES

From the previous discussion it is clear that the most critical element in the operation of the alpha cell is the grid. Its presence is a fundamental principle of operation, but by the same token an improperly designed grid can negate the usefulness of the concept. It is the purpose of this section of the report to present the existing technology of grid design relating to the alpha cell. This can perhaps best be done by considering first-order principles for grid design and then discussing principles relating to second order effects, many of which must be evaluated experimentally.

First-Order Design Principles

To first-order principles, grid design is related to two parameters: the f-factor and the effective amplification factor (or μ-factor), which is the ratio of anode voltage to the grid voltage required to maintain this prescribed anode voltage. In the discussion which follows, it is convenient to describe grid design in terms of a coaxial cylinder geometry, with a squirrel-cage grid around the cathode, but the design principles obviously apply to other geometries.

f-Factor

As previously defined, the f-factor is the fraction of alpha particles escaping the cathode which strikes the grid. Since current losses due to the presence of the grid are proportional to $f(1 + x\,\eta_g)$, i.e., directly proportional to f, and since the magnitude of the k factor is also related to the magnitude of f, it is important that the grid have a small f-factor.

To a first approximation, the f-factor for a long squirrel-cage grid is simply the fractional area of the grid circle cylinder blocked by the grid wires,

$$f \cong \frac{N d_g}{2\pi r_g} \quad , \tag{25}$$

where N = number of grid wires

d_g = diameter of wires

r_g = radius of grid cage circle.

A more refined analysis shows that for finite cathode radius the f-factor is slightly larger than the simple area ratio of Equation (25). To a good approximation the f-factor is given by

$$f = \frac{N d_g \theta}{6\pi^2} \left[\frac{1}{(r_g - r_c)} + \frac{4}{g} + \frac{1}{(r_g^2 - r_c^2)^{1/2}} \right] , \tag{26}$$

where

r_c = cathode radius

$$\cos\theta = \frac{r_c}{r_g}$$

$$g = r_c \left[\frac{1 - \cos\theta}{2} + \left(\frac{1}{\cos\theta} - \sqrt{\frac{1 + \cos\theta}{2}} \right)^2 \right]^{1/2} .$$

This approximation is valid under the conditions that

$$\tan\left(\frac{d_g}{r_g - r_c}\right) \cong \left(\frac{d_g}{r_g - r_c}\right) \text{ and } L >> 2 (r_g - r_c),$$

where L is the length of the grid wires. It can be seen that as r_c approaches zero, the more complex relation of Equation (26) approaches the simple area ratio of Equation (25). The difference in the two equations can be illustrated by the grid used in the initial alpha cell experiments. With $N = 40$, $d_g = 0.010$ in., $r_g = 0.625$ in., and $r_c = 0.250$ in., the area ratio gives $f = 0.113$, compared with $f = 0.120$ from Equation (26); the true f-factor is about 6 per cent larger than the area ratio for this case.

For normal operating grid voltages, the f-factor is purely a geometrical factor. However, for very large grid voltages, the grid (at negative bias) attracts alpha particles and hence the f-factor increases with voltage. An approximate expression for the voltage dependency of the f-factor is

$$f = f_o \sqrt{1 + \frac{Z_o V_g}{E_o}} \quad , \tag{27}$$

where

f_o = geometric f-factor as calculated from Equation (26)

Z_o = charge on the alpha particle

E_o = energy of the alpha particle in electron volts.

Since (E_o/Z_o) is of the order of 10^6, V_g must be of the order of 10^5 volts for this correction to become significant.

Amplification Factor

The amplification factor is the magnitude of the ratio of anode voltage to the grid voltage required to maintain this prescribed anode voltage. Thus, a grid with high amplification factor requires a small bias to suppress the secondary electrons formed at the cathode in the presence of a large anode voltage. This, in turn, alleviates the problem of high voltage gradients across the electrical insulators between the grid and cathode or, alternatively, permits the grid to be located closer to the cathode (since it can operate at low voltage), resulting in a more compact device. Unfortunately, as will be shown, a high amplification factor is generally associated with a large f-factor grid, which lowers the efficiency of the device. Thus, optimum conditions must be sought in the grid design.

In an ordinary triode electron tube, the amplification factor is the ratio of the plate voltage to the negative of grid voltage for a condition of cutoff. In terms of the electric field within the tube, cutoff exists when the gradient of the potential at the cathode is zero.[4] From analysis by Spangenberg, the resulting amplification factor (or mu-factor) for a cylindrical squirrel-cage grid is[5]

$$\mu = \frac{-N \ln\left(\frac{r_p}{r_g}\right)}{\ln\left[2 \sin\left(\frac{Nd_g}{4r_g}\right)\right]}, \tag{28}$$

where r_p is the radius of the anode (plate). This equation is valid for triode tubes with screening fraction approximately 0.1 or less. [The screening fraction is the ratio of grid wire diameter to grid wire spacing, or simply the f-factor as calculated from Equation (25).] For most grid designs of interest, $\sin\left(\frac{Nd_g}{4r_g}\right) \cong \left(\frac{Nd_g}{4r_g}\right)$ so that Equation (28) can be simplified to

$$\mu = -\frac{N \ln\left(\frac{r_p}{r_g}\right)}{\ln\left(\frac{Nd_g}{2r_g}\right)} \cong \frac{N \ln\left(\frac{r_p}{r_g}\right)}{\ln\left(\frac{1}{\pi f}\right)}. \tag{29}$$

To a first-order approximation, this definition of amplification factor may be used in designing the alpha cell. The principal approximation comes about by neglecting the initial energy of the secondary electrons.

By inspection of Equation (29), it is seen that the amplification factor increases with the number of grid wires, since N appears as a linear factor in the numerator whereas it is only as a logarithmic factor in the denominator. It also increases with anode radius and grid-wire diameter. The amplification factor decreases as the radius of the grid cage increases. This equation can be used in conjunction with (25) or (26) to optimize the relation between μ and f if several of the variables are fixed by other restrictions. For example, Cranberg's criterion for voltage breakdown in vacuum[6] determines the spacing required between the grid and anode. Also, required structural strength of the grid can restrict the values of the grid-wire diameter.

Second-Order Effects Influencing Grid Design

Although the f-factor and amplification factor are critical to grid design, several other factors may have significant influence on grid design. Examples of such factors are

(1) Dependence of secondary-electron yield at the grid on grid-wire material. [Since losses are proportional to f $(1 + x \eta_g)$, in addition to minimizing f, it is desirable to choose grid wire material to minimize η_g, or hence the secondary electron yield at the grid, $\Delta_g = Z \eta_g$.]

(2) Dependence of secondary yield on electric field. For secondaries produced at the grid wires at locations exposed to the anode field, a significant increase in Δ_g might occur because of the electric field. Depending on the importance of this effect, it might be desirable to stagger the distance of the grid wires from the cathode.

(3) Gamma-induced secondary electron emission. For alpha emitters, such as polonium-210, which have very weak associated gamma radiation, the electron production due to the gamma radiation can generally be ignored. A small effect due to gamma-induced secondary emission at the grid wires might be observable for alpha emitters with appreciable associated gamma radiation, such as curium-244. The emission for metals is of the order of 0.5×10^{-16} amp/cm^2 per roentgen/hr.[7, 8]

(4) Bremsstrahlung production. The leakage current from grid to anode due to secondary-electron production at the grid constitutes a source of bremsstrahlung at the anode. The electrons leaking from the grid are accelerated by the anode field to energy equivalent to the anode voltage, and hence strike the anode with energy of the order of 1 Mev. The leakage current, and hence the bremsstrahlung production, is proporational to $(xf\eta_g)$, i.e., directly proportional to f. The radiation thus produced, in addition to presenting a possible hazard, can in turn produce secondary emission of magnitude discussed in Item (3).

(5) Structural strength of grid. At large anode voltage, the electrostatic force of attraction between anode and grid is sufficiently strong to deflect the grid wires if they are constrained only at the ends of the grid. Use of containing rings spaced along the squirrel-cage grid minimizes this deflection.

SPACE-CHARGE LIMITATION

It is to be expected that the limitation imposed on the current in the alpha cell because of space-charge effects is not a serious one since the alpha cell is basically a low-current, high-voltage device. A brief analysis of the space-charge-limited current in a simplified geometry is presented here to illustrate the magnitude of the effect.

The basic relations for charge flow at equilibrium in a space between two conductors are (in MKS units)

Poisson's equation: $$\nabla^2 V = -\rho/\epsilon_o \tag{30}$$

Continuity equation: (conservation of charge) $$\underline{\nabla} \cdot \underline{J} = 0 \tag{31}$$

Conservation of energy: $$E_o = \left(\frac{1}{2}\right) Mv^2 + Z_o V, \tag{32}$$

where the current density $\underline{J}$ is given by

$$\underline{J} = \rho \underline{v} , \tag{33}$$

and where ρ = charge density

$\underline{v}$ = alpha-particle velocity

M = mass of alpha particle (of initial energy E_o and charge Z_o)

ϵ_o = permittivity of free space

V = voltage

For simplicity the geometry used in this analysis is that of two infinite parallel-plane electrodes spaced a distance x_o apart. In this geometry, V, ρ, and v are functions of x only. The current flow per unit area from the emitter is the x-component of $\underline{J}$. Only the kinetic energy E_{ox} associated with the x-component of the velocity is transformed into potential (electrostatic) energy; the remaining energy is dissipated at the cathode.

The boundary conditions to be applied to the solution to the basic relations (30) through (32) are

$$V(0) = 0$$
$$\left(\frac{dV}{dx}\right)_{x = x_o} = 0 \tag{34}$$

This second condition is an approximation based on the fact that the large number of positive ions in the neighborhood of the collector ($x = x_o$) neutralizes the field in this region. That there is a buildup of ions near the collector is seen from the solution to Equation (31) that $J_x = \rho v_x$ = constant, and since the kinetic energy is dissipated in overcoming the potential barrier, near the collector v_x is small so that ρ must be large.

The general solution to the problem is the implicit relation

$$\left(\frac{J_x Z_o \sqrt{\frac{M}{2}}}{4\epsilon_o}\right)^{1/2} x = \frac{1}{3}\left\{\left[E_{ox}^{1/2} - (E_{ox} - Z_o V_A)^{1/2}\right]^{3/2}\right.$$

$$- \left[(E_{ox} - Z_o V)^{1/2} - (E_{ox} - Z_o V_A)^{1/2} \right]^{3/2} \Bigg\}$$

$$+ (E_{ox} - Z_o V_A)^{1/2} \left\{ \left[E_{ox}^{1/2} - (E_{ox} - Z_o V_A)^{1/2} \right]^{1/2} - \left[(E_{ox} - Z_o V)^{1/2} - (E_{ox} - Z_o V_A)^{1/2} \right]^{1/2} \right\} , \quad (35)$$

where V_A is the collector (anode) voltage. At $V = V_A$ (at $x = x_o$), Equation (35) simplifies to

$$\left(\frac{J_x Z_o \sqrt{\frac{M}{2}}}{4\epsilon_o} \right)^{1/2} x_o = \frac{1}{3} \left[E_{ox}^{1/2} - (E_{ox} - Z_o V_A)^{1/2} \right]^{3/2}$$

$$+ (E_{ox} - Z_o V_A)^{1/2} \left[E_{ox}^{1/2} - (E_{ox} - Z_o V_A)^{1/2} \right]^{1/2} . \quad (36)$$

To obtain an estimate of J_x from this expression, it is assumed that $V_A = \frac{E_{ox}}{Z_o}$. With this value of anode voltage, the cathode current density is

$$J_x = \left(\frac{4\epsilon_o \sqrt{\frac{2}{M}}}{9 Z_o} \right) \left(\frac{E_{ox}^{3/2}}{x_o^2} \right) . \quad (37)$$

This represents the maximum current density that can be obtained for a given spacing at full anode voltage, i.e., this is the space-charge-limited current. (A larger current is obtained if the anode voltage is reduced from the maximum possible value of E_{ox}/Z_o.)

The magnitude of the space-charge-limited current may be estimated by assuming the following "typical" values for the parameters

$E_{ox} = \frac{1}{3} E_o = 1.7$ Mev $= 2.7 \times 10^{-13}$ nt-m

$Z_o = 2e = 3.2 \times 10^{-19}$ coul

$X_o = 10$ cm $= 0.1$ m

$M = 4$ amu $= 6.6 \times 10^{-27}$ kg

$\epsilon_o = 8.85 \times 10^{-12}$ coul^2/nt-m^2

which gives $J_x = 3 \times 10^3$ amp/m^2 $= 0.3$ amp/cm^2. At the assumed voltage, this is equivalent to a power density of 250,000 watts/cm^2! This large value for J_x, and hence for the power density, indicates that space-charge effects are negligible for the alpha-cell concept. A typical alpha-cell system might operate at a current density of about 10^{-7} amp/cm^2. Such conditions are seen to be a factor of 10^6 below the limitations set by space-charge effects.

The limiting current for a cell with cylindrical or spherical geometry is greater than that for the parallel planes, with the same electrode spacing. Since the limiting current was so large in the case considered, the other geometries were not considered in detail.

MAGNETIC SUPPRESSION OF SECONDARY ELECTRONS

An alternative method of suppressing the secondary-electron emission accompanying the emission of alpha particles from the cathode is the application of an axial magnetic field. Such an arrangement would eliminate the efficiency loss due to the presence of the grid. However, as will be shown from the analysis summarized below, the intensity of magnetic field required for effective secondary-electron suppression in the presence of a megavolt anode potential is of the order of 1000 gauss and thus impractically large.

For concentric-cylinder electrodes with the outer electrode (anode) of diameter b and inner electrode (cathode) of diameter a, the electric field produced by anode voltage V_A is

$$\underline{E} = \frac{V_A}{r \ln \left(\frac{a}{b}\right)} \underline{e}_r \tag{38}$$

where r is the radial distance and $\underline{e}_r$ is the unit vector in the radial direction. An electron emitted at the cathode is accelerated to the anode by the force $q\underline{E}$, where q is the electron charge. Since it is desired that only the positively charged alpha particles reach the anode, to prevent electron transfer the magnetic force must oppose and exceed the electrostatic force. An axial magnetic field $\underline{B}$ will produce a force which, if sufficiently large, will curl the electrons back to the cathode. The net force on an electron is then

$$\underline{F} = q(\underline{E} + \underline{v} \times \underline{B}) . \tag{39}$$

Although the electron emission may be isotropic, the magnetic field required for complete suppression must be of sufficient magnitude to return those electrons with initial energy U_s emitted radially. Allowing for relativistic electron energies, Schock[9] derived an expression for the magnitude of the axial magnetic field required to completely turn back electrons of initial energy U_s (in ev):

$$B = \frac{2U_o}{bc\,(1-\beta^2)} \left\{ \left[\left(\frac{U_s + V_A}{U_o} + 1 \right)^2 - 1 \right]^{1/2} + \beta \left[\left(\frac{U_s}{U_o} + 1 \right)^2 - 1 \right]^{1/2} \right\} , \tag{40}$$

where

B = axial magnetic field, webers/m^2

β = a/b

c = velocity of light, m/sec

U_o = rest-mass energy of an electron, ev

V_A = anode voltage.

Since the secondary electrons have energies at birth of the order of a few ev, and nearly all have energy less than 100 ev, the initial energy U_s can be neglected with respect to V_A and U_o.* The magnetic field required to suppress zero-energy electrons (i.e., low-energy secondaries) is given from Equation (40) as

$$B(0) = \frac{2U_o}{bc\,(1-\beta^2)} \left[\left(\frac{V_A}{U_o} + 1 \right)^2 - 1 \right]^{1/2} , \qquad (41)$$

where b, the anode diameter, is expressed in meters.

To obtain an estimate of the magnitude of the magnetic field required to suppress the secondary electrons, β^2 can be neglected compared with unity. Figure 6 is a plot of Equation (41) with this approximation. It is seen that for anode voltages of interest, the product (Bb) must lie in the range of 0.01 to 0.02 weber/m. Thus for anode diameter of 0.2 m (20 cm), an axial field of the order of 0.1 weber/m^2 (1000 gauss) is required.

To obtain a 1000-gauss magnetic field over the volume of an alpha cell is prohibitive from the standpoint of magnet weight and power loss. For these reasons, the choice of a grid to suppress secondary electrons appears to be imperative.

SELECTION OF AN ALPHA EMITTER FOR THE ALPHA-ELECTRIC CELL

Since nearly all alpha emitters occur in the range of high atomic number, the selection of a cathode coating material is limited to those radioisotopes above bismuth (Z = 83) in the periodic table. Although the number of alpha-emitting radioisotopes in this range is large, only a few have half-lives in the range dictated by power and lifetime requirements for a useful system. Assuming the minimum system lifetime of interest to be about 6 months, the lower limit of isotope half-life should be no less than 3 or 4 months. The upper limit of half-life is prescribed by maximum power output required, since these two parameters are inversely related, i.e., as half-life increases, specific power available decreases. Thus, the half-life range of interest is from about 3 months to a few hundred years. The alphas in this limited range of half-lives have similar decay energies, virtually eliminating the need for consideration of this parameter in selecting suitable isotopes for the alpha cell.

A recent survey[10] indicates that the most promising alpha emitters for the concept are polonium-210, curium-242, curium-244 and plutonium-238. Table 2 summarizes the properties and cost of these isotopes. There are several other isotopes with half-lives in the required range, notably californium-248, einsteinium-252, and plutonium-236, but these are so rare as to not be given consideration at this time. Another possible emitter, thorium-228 (half-life 1.9 years), decays as part of the thorium (4n) series and is thus a source of undesirable short-lived beta emitters. In addition it is comparatively rare.

*That the required magnetic field is nearly independent of the initial electron energy U_s is due to the fact that, in the presence of an anode potential of the order of a megavolt, most of the energy of the electron as it moves toward the anode is in the form of an increase in kinetic energy acquired from the electric field.

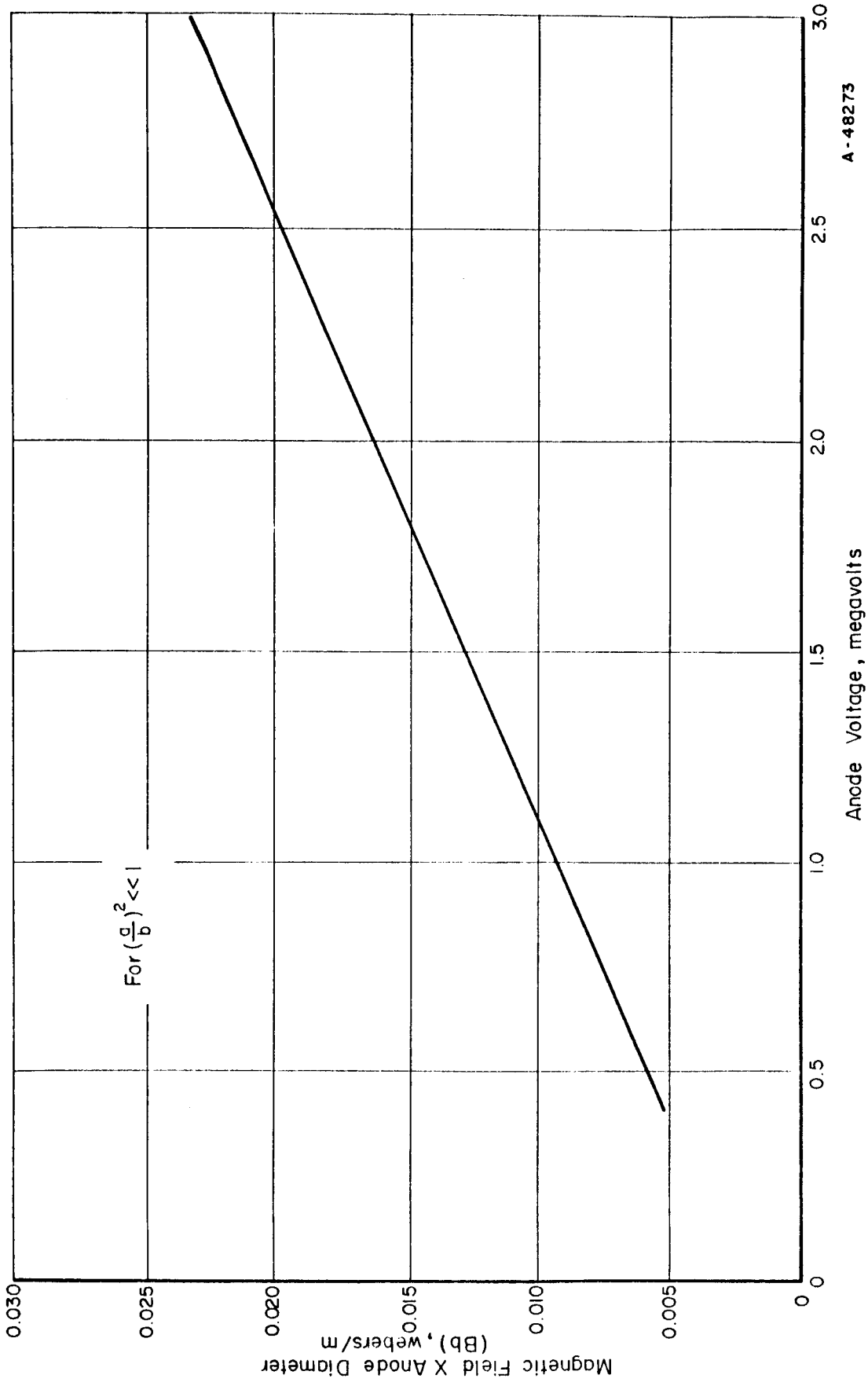

FIGURE 6. MAGNETIC FIELD REQUIRED TO SUPPRESS SECONDARY ELECTRONS

TABLE 2. ALPHA EMITTERS APPLICABLE TO ALPHA-CELL CONCEPT[a]

Isotope	Alpha Energy, Mev	Half-Life, years	Chemical Form	Thermal Power, watts/g	Projected Cost[b], $ per thermal watt
Polonium-210	5.3	0.38	Metal	140	190
Plutonium-238	5.5	90	Metal	0.48	1040
Curium-242	6.1	0.44	Oxide	120	165
Curium-244	5.8	18	Oxide	2.3	435

(a) Most data from Reference (10).
(b) Polonium-210 is the only isotope currently available in large quantity. Its present cost is $640 per thermal watt.

Along with the emergence of alpha-particles from the emitters listed in Table 2 come gamma rays, which present a low-level shielding problem. In addition secondary reactions, or in some cases spontaneous fission, provide a source of neutrons. Table 3 summarizes the radiation from 100-watt (thermal) bare alpha sources for the first three isotopes of Table 2. As seen from these data, the two short-lived isotopes have comparable radiation attendant their use. The radiation from plutonium-238 is about two orders of magnitude less.

TABLE 3. RADIATION FROM 100-WATT (THERMAL) BARE ALPHA SOURCES[a]

Isotope	Gamma Radiation, millirem/hr at 1 yard	Neutron Radiation, millirem/hr at 1 yard	Total Radiation, millirem/hr at 1 yard
Polonium-210	20.0	6.5	26.5
Curium-242	4.3	32.5	36.8
Plutonium-238	0.01	0.53	0.53

(a) Data from Reference (10).

It is apparent from this brief survey of available emitters that mission lifetime will be the principal factor in dictating the selection of alpha emitter from the four listed in Table 2. Only for the short mission is a choice really available (polonium-210 versus curium-242).

EXPERIMENTAL STUDIES

This section of the report describes the experimental studies performed with the alpha cell and summarizes the results. Prior to the initiation of the study under contract with NASA, preliminary experiments aimed at demonstrating proof of principle were performed under Battelle sponsorship. These are summarized briefly to provide the background for a discussion of the more recent results.

RESULTS OF BATTELLE SPONSORED EXPERIMENTS

Preliminary Measurements of Secondary-Electron Emission

During the early conceptual stage of the development of the alpha electric cell, it was postulated that the key to efficient operation would be the use of a properly designed grid interposed between the emitter and collector electrodes. It was further anticipated that the cell simply would not work (i. e., there would be no voltage buildup) without a grid, because of an excessive number of secondary electrons emitted as each alpha particle emerges from the source material. There was no direct experimental evidence to support this belief, although results of early investigations with alpha-particle-induced secondary emission, summarized by H. Geiger[11], indicated yields in the range of 3 to 30 for alpha-particle bombardment of a metal surface. However, the foundation was still sufficiently lacking and warranted a preliminary experiment prior to design and construction of a more complex and expensive experiment in the form of an actual alpha electric cell.

For the preliminary experiment, a small polonium source (2. 5 millicuries at the time of the experiment) was placed in a vacuum chamber, and the emission current measured. The polonium was deposited on a copper backing in a circular area approximately 1 cm in diameter. The source was flashed with a thin gold coating to prevent migration of the polonium and subsequent contamination of the experiment. The secondary-electron emission as the alphas emerge from the gold coating should be similar to that produced by polonium alone (of equivalent thickness), since both elements have similar mass stopping powers for alphas. From measurement of the average energy of the alphas emerging from the source, it was estimated that the gold thickness was about 3 microns. The source was supported in the vacuum facility on an aluminum pedestal electrically insulated from the baseplate.

The emission current was measured as the source was maintained at various negative voltages with respect to the vacuum chamber dome. Data were obtained with and without the source. By subtracting the currents measured under these two conditions, leakage and other extraneous currents were eliminated. The results are shown graphically in Figure 7. With sufficiently large negative bias on the source to return secondary electrons produced at the wall of the vacuum chamber (>400 volts), the source current was measured to be 3.2×10^{-11} ampere. Scatter in the data is attributed principally to the large contribution of background current. To obtain the source current, the data above 400 volts were averaged.

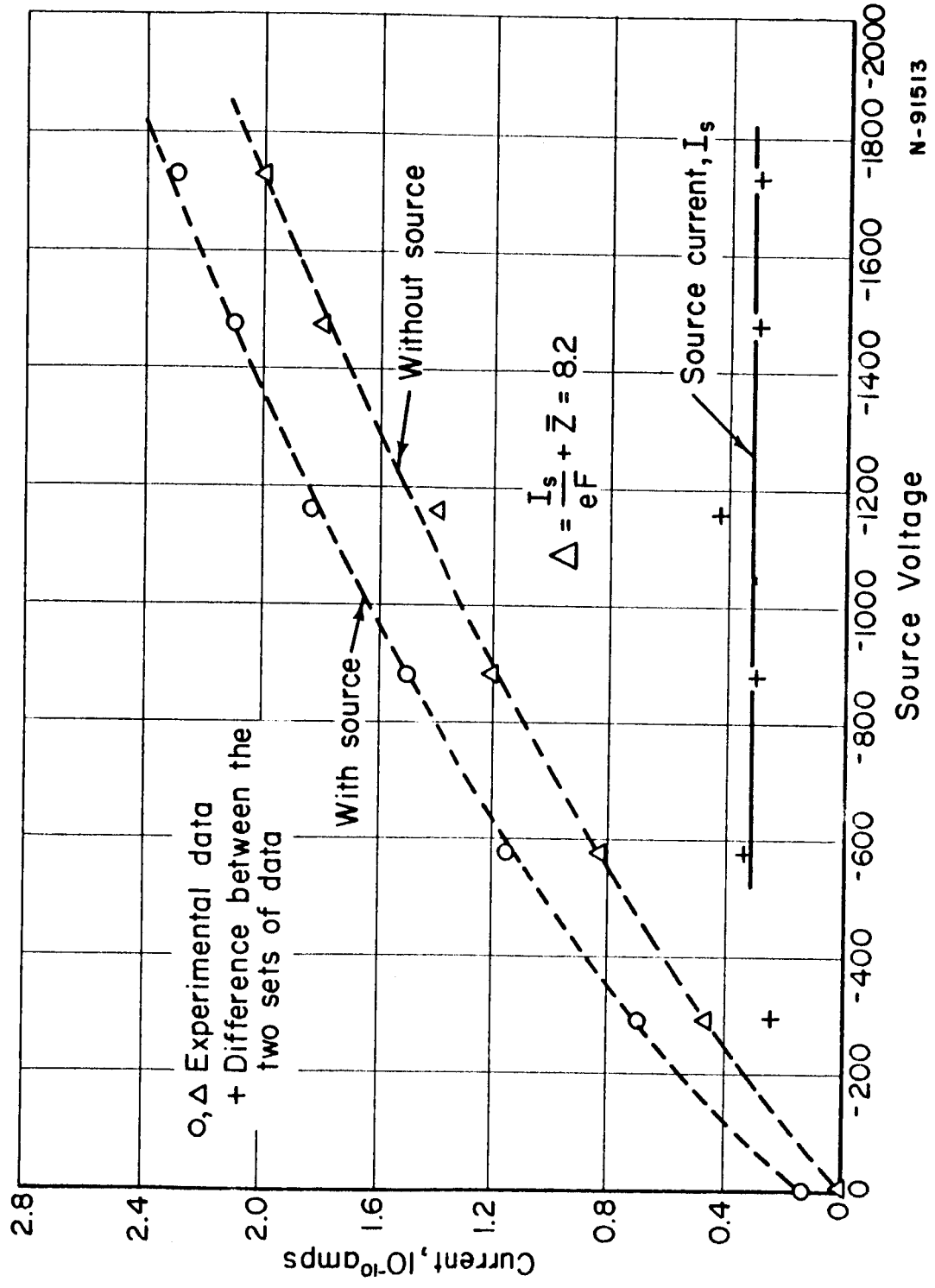

FIGURE 7. SOURCE-CURRENT MEASUREMENT FOR PRELIMINARY EXPERIMENT

Under the conditions of the experiment, the secondary-electron yield is

$$\Delta = \frac{I_s}{eF} + \overline{Z} , \tag{42}$$

where

I_s = magnitude of the current leaving the source, amperes

$\overline{Z}$ = average charge of an escaping alpha particle

F = number of alpha particles leaving the source per unit time.

$$F = \frac{F_o}{2}\left(1 - \frac{t}{R}\right), \tag{43}$$

where F_o is the disintegration rate in the polonium, t is the thickness of gold, and R is the mean range of alpha particles in gold.* With t/R approximately 0.3, for the 2.5-millicurie source $F = 3.2 \times 10^7$ alphas/second. Since t/R is rather small, to a first approximation it may be assumed that the alpha particles retain their charge of +2. Since the first term in the yield equation is the larger term, the fact that the average charge may be degraded does not seriously affect the results. With these values of F and $\overline{Z}$, and the measured value of $I_s = 3.2 \times 10^{-11}$ ampere, the secondary-electron yield was determined to be 8.2, i.e., on the average 8.2 secondary electrons are emitted as each alpha particle emerges from the surface.

From this preliminary experiment it was concluded that the charge carried by the secondaries is larger than the opposing charge carried by the alphas, verifying the statement that a grid is essential to the operation of the device. On the other hand, the yield is not so large as to magnify the problem of current loss due to secondary-electron production at the grid. (As discussed previously, loss in alpha-particle charging current is proportional to $(1 + x\Delta_g/\overline{Z})$, where Δ_g is the secondary-electron yield due to a small fraction of alpha particles striking the grid, and x is the fraction of secondaries formed at the grid which escape to the anode.)

The next step in the demonstration of the feasibility of the concept was to construct an actual cell and prove that with proper grid bias a voltage buildup could be obtained.

Initial Experiments With the Alpha Cell

The preliminary proof-of-principle experiments using a polonium alpha emitter were performed in late 1962. Figure 8 shows photographs of the experimental apparatus. The picture to the left shows the grid-cathode assembly used in these experiments. Several curies of polonium-210 were distributed uniformly on a cathode 1/2 inch in diameter by 12 inches long. To minimize contamination of the equipment a thin gold foil (0.0001 inch thick) was wrapped over the bare polonium surface. The cathode was surrounded by a squirrel-cage grid of 40 stainless steel wires 10 mils in diameter equally spaced on a 1.25-inch-diameter grid circle and supported at the ends. As shown by the second photograph in Figure 8, the grid-cathode assembly was installed

*For the source used in this experiment, the thickness of the polonium itself is much less than that of the gold layer deposited on top of the polonium. The above formula for F consequently differs from the usual relation $F = F_o/2\,(1 - t/2R)$ for a coating in which the alpha particles are born uniformly throughout the coating material.

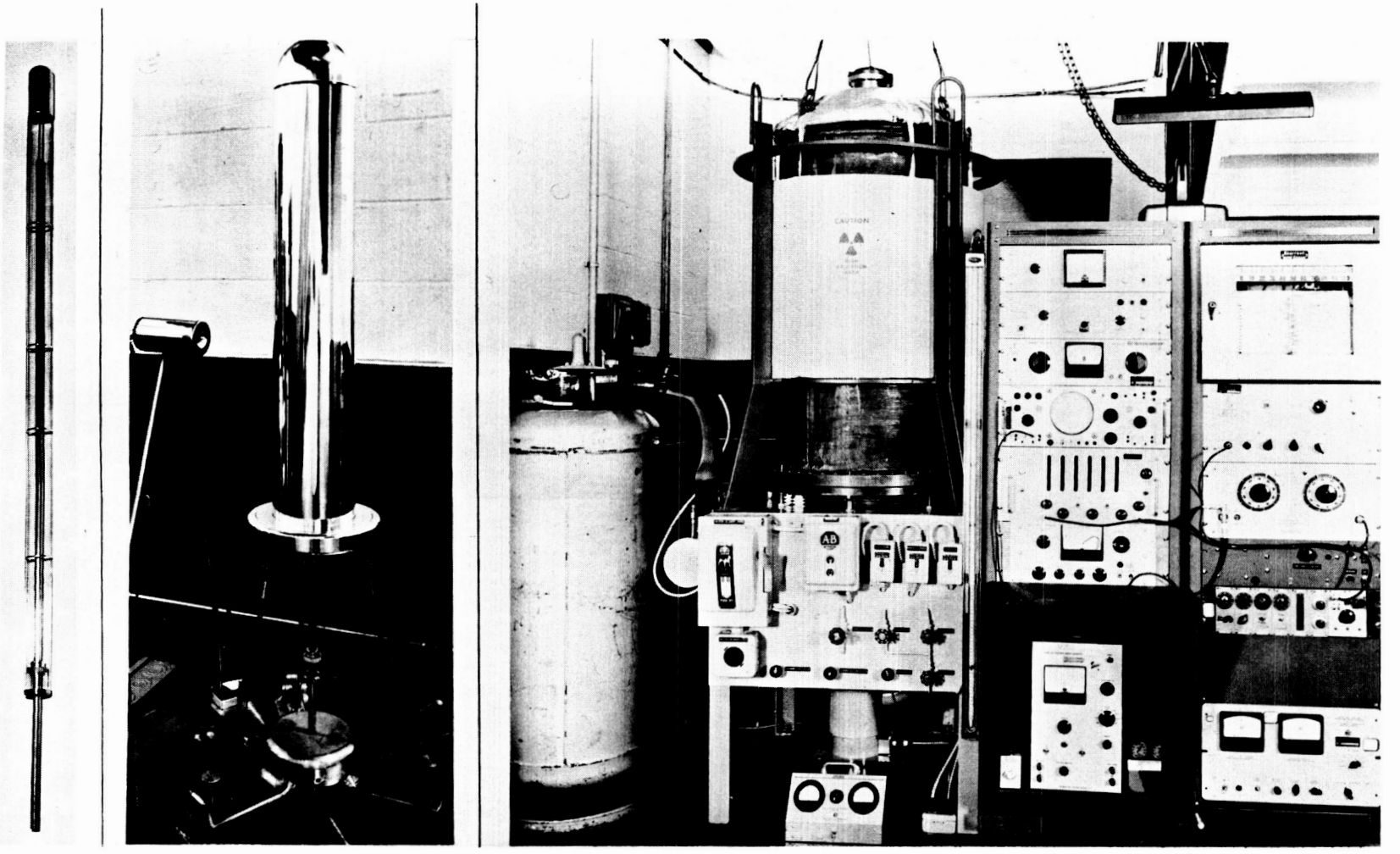

Grid-Cathode Assembly

Anode

High-Vacuum Facility and Instrument Console

N93983

FIGURE 8. EQUIPMENT FOR ALPHA-ELECTRIC-CELL EXPERIMENTS

into a concentric 4-inch-ID anode cylinder electrically insulated by a quartz tripod. A vacuum chamber lowers over the apparatus and fastens to the base plate. This picture also shows the components of the high-voltage measuring apparatus. The measurement of anode potential is complicated by the fact that the measurement must be made without appreciable current drain and that the voltage information must be transmitted outside the vacuum. Considerable effort was devoted to a study of different methods for voltage measurement until a satisfactory method was found. This method determines the anode voltage by measuring the increase in energy of an alpha particle accelerating through the electric field set up by the anode. Descriptions of this technique are given in the literature.[12, 13]

For the measurements, a 2-millicurie polonium-210 alpha source was mounted on the outer surface of the anode. A small gas-filled chamber (with variable gas pressure) containing a thin mica window and a silicon-gold charged-particle solid-state detector was placed so that the detector could "see" the alpha source through the mica window. The small chamber was vacuum-sealed and connected by a 1/4-inch line through the test-chamber base plate to a separate evacuating system. With this arrangement the pressure in the small chamber could be varied from a few microns to 1 atmosphere without affecting the vacuum in the large test dome. Measurements with the solid-state detector as the pressure was varied in the small chamber determined the range in air of the alpha particles from the anode. From the measured range and the well-known range-energy relationships[14], the energy of the alpha particle could be determined. The anode voltage is then simply the energy at this voltage minus the energy with the anode grounded divided by the charge on the alpha particle. This technique has the advantages that the measured energy increment, ΔE, is not very sensitive to either the initial energy of the alpha particle or the physical dimensions of the detector. While it is true that the voltage determination comes from taking the difference between two large numbers, analysis of the data and techniques indicate an accuracy of better than ±10 per cent at 10^5 volts and higher. This accuracy is competitive with any other high-voltage measurement in the 10^5 to 10^6-volt range. By use of a ratemeter, the technique was converted to a continuous high-voltage measuring device.

The photograph to the right in Figure 8 shows the vacuum test chamber and the instrumentation associated with the initial alpha-cell experiment. The vacuum chamber is a stainless steel bell jar 24 inches in diameter and 56 inches high which seals to a stainless steel base plate. The chamber is evacuated by a 6-inch oil-diffusion pump backed by a 46-cfm forepump. A 6-inch chevron cold trap (liquid-nitrogen cooled) is mounted on top of the diffusion pump and sealed almost directly into the base plate. With this arrangement pressures in the 10^{-8} mm Hg range are readily attainable. A 4-inch quartz window is sealed into the top of the vacuum dome for visual observation of the experiment.

Voltage Buildup Experiments

To determine the high-voltage-buildup limits of the apparatus, prior to inserting the alpha source a special anode was installed on the quartz tripod inside the vacuum chamber with small cerium-144 – praseodymium-144 beta sources attached to the top of the anode. With beta emission, the anode charged up to 50,000 volts. At this voltage, microdischarging was initiated which abruptly termined further voltage buildup. Thus, prior to the alpha experiments, it was determined that the apparatus was capable of sustaining 50,000 volts without breakdown.

Voltage buildup with the alpha cell was measured for a variety of grid biases. A maximum of 50,000 volts was obtained in these initial experiments, which was the upper limit of the equipment and sufficient to prove the principle of operation. A grid voltage of -800 volts was sufficient to maintain this potential. It was observed that microdischarges were again responsible for the limitation in voltage buildup. Observations have shown that this microdischarging is a threshold phenomenon, i.e., essentially no microdischarges occur until the voltage attains a critical value, at which voltage the microdischarging is initiated with a frequency such that the current leakage in the discharging just matches the charging current.

Alpha-Cell Currents

Measurements in the initial experiments included a determination of cell currents as a function of grid bias at zero anode voltage. The predictions for cell currents were derived previously and illustrated in Figure 4. Below a few hundred volts on the grid, the energy distribution of the secondary electrons will affect the currents, but at high negative grid bias, the grid and cathode currents should be independent of grid bias. From the previous analysis, the cathode current would be expected to be larger than the alpha-particle current by an amount $(1 - x) f\eta_g I_o$, which represents a flow of secondary electrons formed at the grid back to the cathode. Of course, it would be hoped that the grid current is small enough that a positive net current is obtained from the device, i.e., $I_{cathode} + I_{grid} > 0$.

The measured currents are shown in Figure 9. As seen from these data, the cell currents were found to behave very nearly as expected in the ideal case. At grid bias greater than -500 volts, the currents are essentially independent of changes in grid voltage. The cathode (I_{co}) is greater than the net current (I_c), and the charging current I_c (the net from the grid-cathode assembly) is a positive current so that buildup of anode voltage could be expected.

Other Experimental Results

Energy Distribution of Secondary Electrons. The energy distribution of secondary electrons formed at the cathode as the alpha particles emerge is reflected by the grid-bias curve shown in Figure 10. As seen from these data, more than half of the secondary electrons produced by the alpha particles are collected at the grid with a positive potential of 10 volts and nearly all are collected with 100 volts on the grid. This general behavior is consistent with observations that the most probable energy of the secondary electrons is 4 to 10 ev.

Secondary-Electron Yield. From a detailed study of the currents in the alpha cell, the secondary-electron yield was determined to be 9.2 electrons for each alpha particle emerging from the thin gold layer covering the polonium on the cathode.[3] This yield determination is a refinement of the measurement performed in the preliminary study discussed previously and indicates that the early value of 8.2 was a fair approximation to the actual yield.

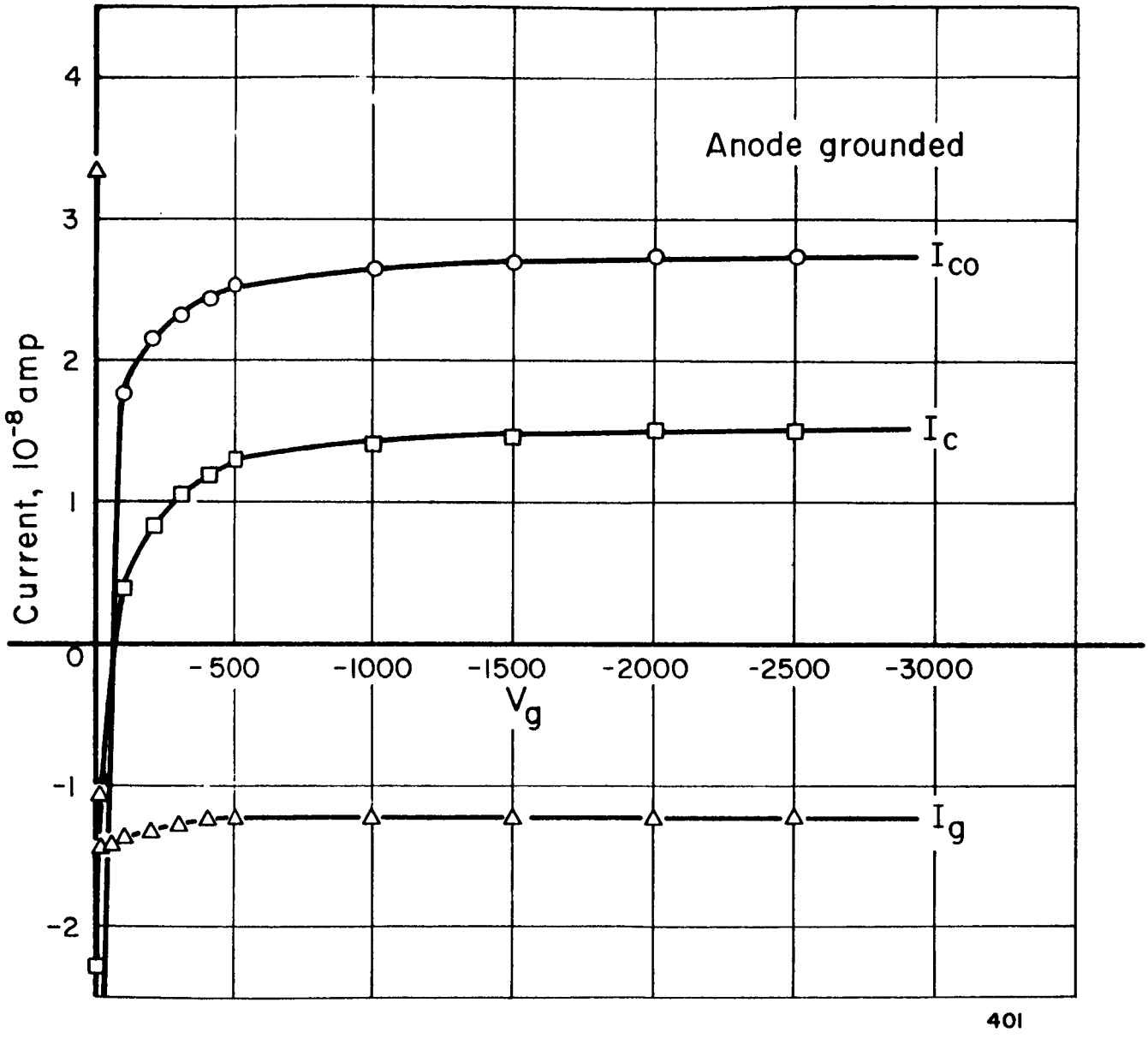

FIGURE 9. ALPHA-ELECTRIC-CELL CURRENT-VOLTAGE CURVES FOR NEGATIVE GRID BIAS

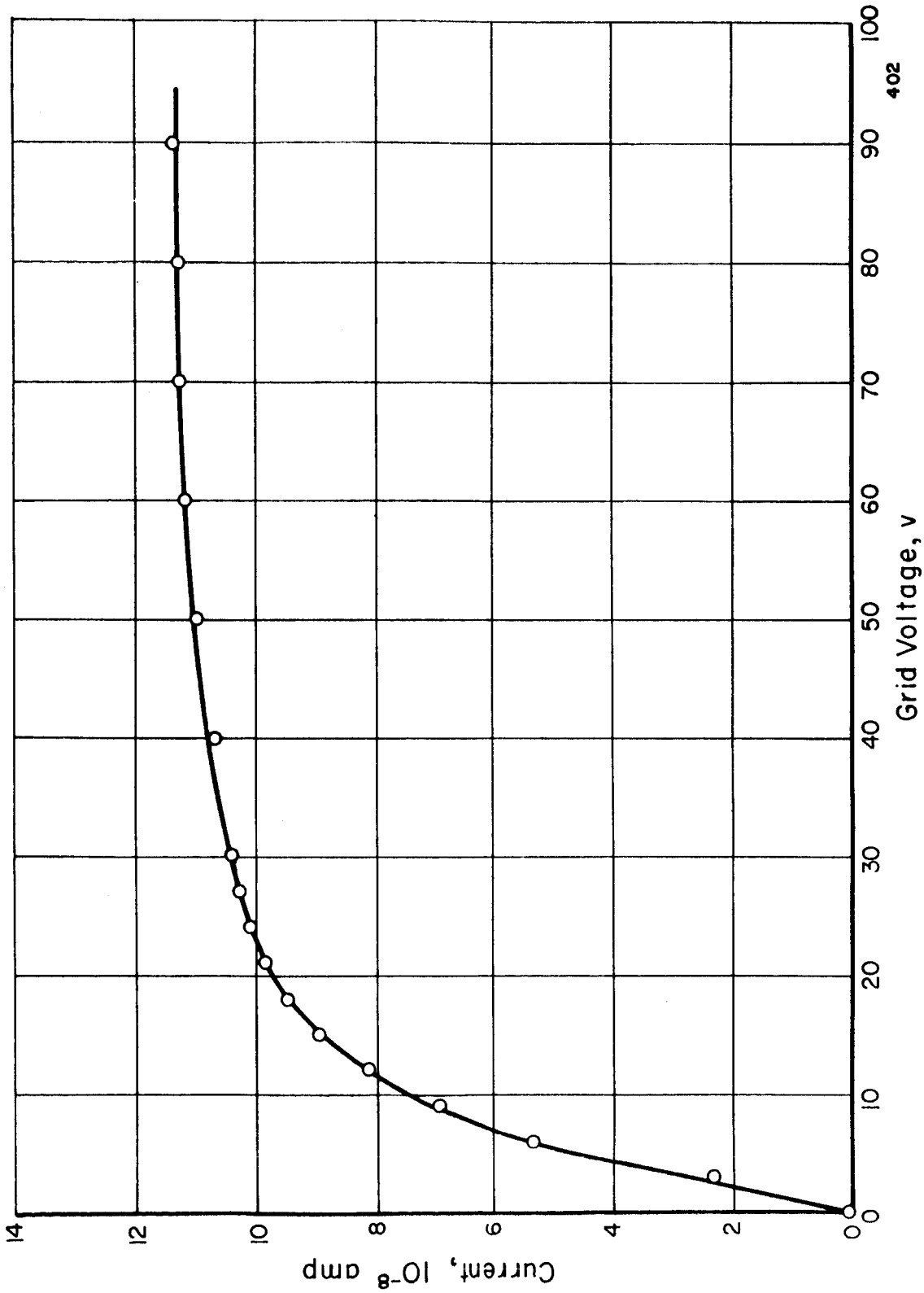

FIGURE 10. GRID CURRENT VERSUS GRID BIAS FOR POSITIVE GRID BIAS, ZERO ANODE VOLTAGE

Effect of Pressure on Voltage Buildup. The effect of test-chamber pressure on the maximum voltage buildup was briefly examined and some rather interesting phenomena observed. Figure 11 shows the effect of pressure on voltage buildup when using a beta emitter to charge up the anode. As seen from these data, the anode voltage was independent of pressure below about 10^{-4} mm Hg. Between 10^{-4} and 10^{-3} mm Hg the voltage dropped to zero. Then at 10^{-3} mm Hg it increased rapidly to about twice the high-vacuum value. Further increase in pressure caused a rapid decrease to zero voltage again. This rather anomalous behavior is roughly the same as that which was observed by Linder and Christian at RCA with a beta emitter.[2] The peak in voltage may be due to a surface-condition effect on secondary-electron and ion emission. The rapid decrease in voltage above 10^{-3} mm Hg is apparently due to ionization of the gas.

The same experiment was repeated with the alpha cell, with results as shown in Figure 12. As seen from these data, again below 10^{-4} mm Hg pressure the anode voltage was constant. The behavior above 10^{-4} mm Hg was qualitatively the same as observed with the beta device, i.e., with increasing pressure, the voltage first decreased, then peaked and finally dropped to zero above 10^{-3} mm Hg. However, near 10^{-3} mm Hg a few gross discharges were observed, and the pressure-voltage curve contained additional peaks.

Except for these studies of voltage behavior with pressure, all experiments were performed at pressures of about 10^{-7} to 10^{-6} mm Hg pressure. However, it appears from these data that only 10^{-4} mm Hg pressure is required for the operation of the alpha cell. This study was limited, of course, to the 50,000-volt range obtained in these initial experiments.

Amplification Factor of Grid. The ability of the theoretical expression for amplification factor, μ, in a triode electron tube, Equation (28), to describe the amplification factor of the grid in the alpha cell was checked experimentally during the initial experiments. The purposes of this particular experiment were twofold: to determine if grid bias was limiting voltage buildup and to obtain a measurement of the amplification factor of the grid. Maximum anode voltage was measured as a function of grid bias. The data are shown graphically in Figure 13. As seen from these data, grid bias was not limiting voltage buildup; rather, voltage buildup was limited by microdischarges as discussed previously. Over the grid-voltage range where the grid bias is the limiting factor (up to -800 volts), a rough measure of the amplification factor can be obtained. Due to the inability to accurately measure low voltages with the alpha-particle voltage-measuring technique, there is considerable scatter in the data. Although there may be a nonlinear behavior in the curve of anode voltage V_A versus grid voltage V_g, a gross measure of μ is given as $\mu = \Delta V_A / \Delta V_g \cong 50$. This value compares favorably with the value of 41 calculated from Equation (28). Although experiments at higher voltages must be relied upon to obtain a more accurate comparison, it appeared from this study that the theoretical prediction is sufficiently valid for preliminary design purposes.

Microdischarges

The data on the amplification-factor measurement shown in Figure 13 emphasize the effect of microdischarges on limiting voltage buildup in the alpha cell. The present theoretical and experimental status of high-voltage breakdown across a vacuum gap indicates that a critical current of the order of 10^{-4} amp is required to initiate

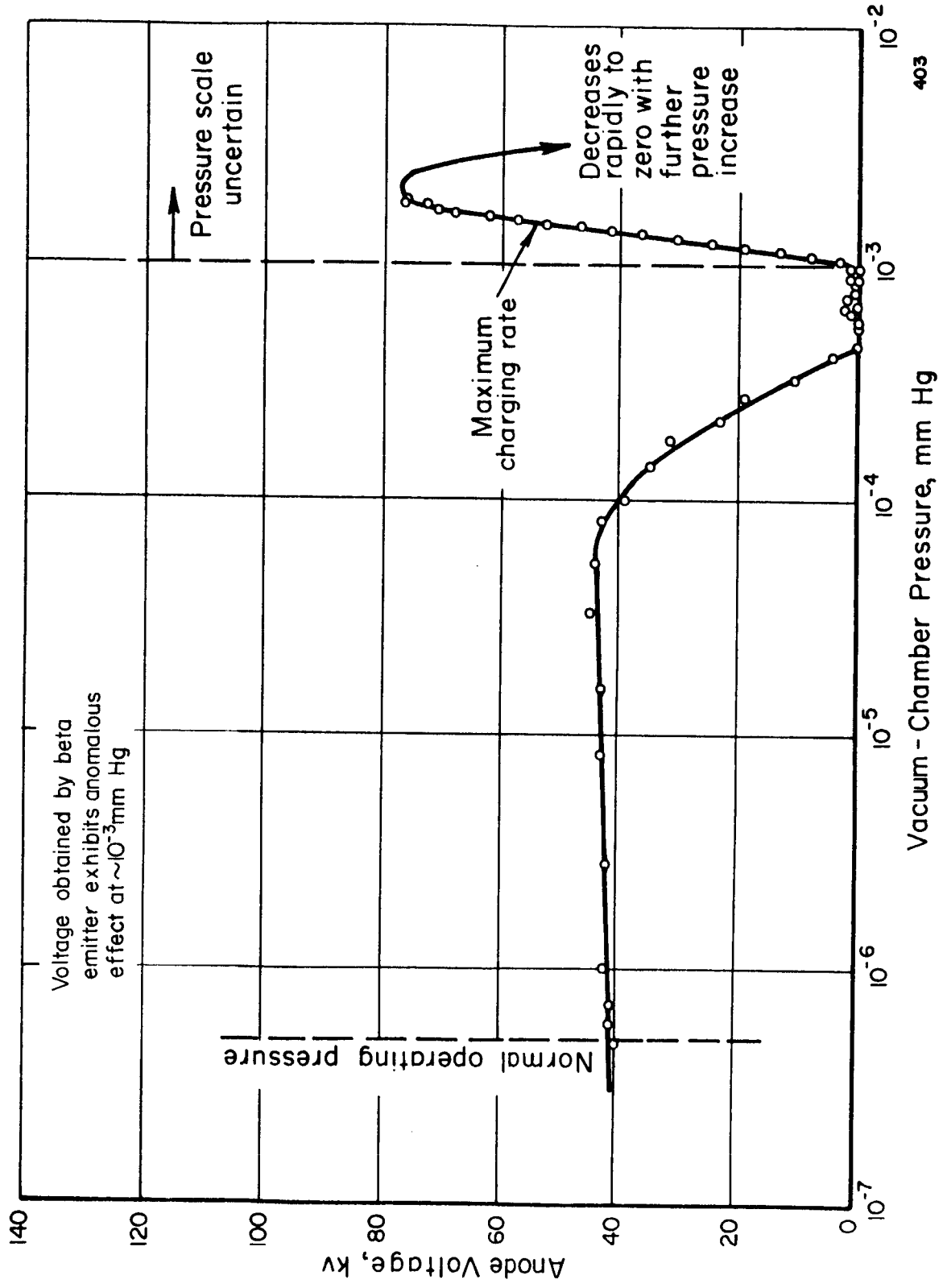

FIGURE 11. ANODE VOLTAGE VERSUS PRESSURE

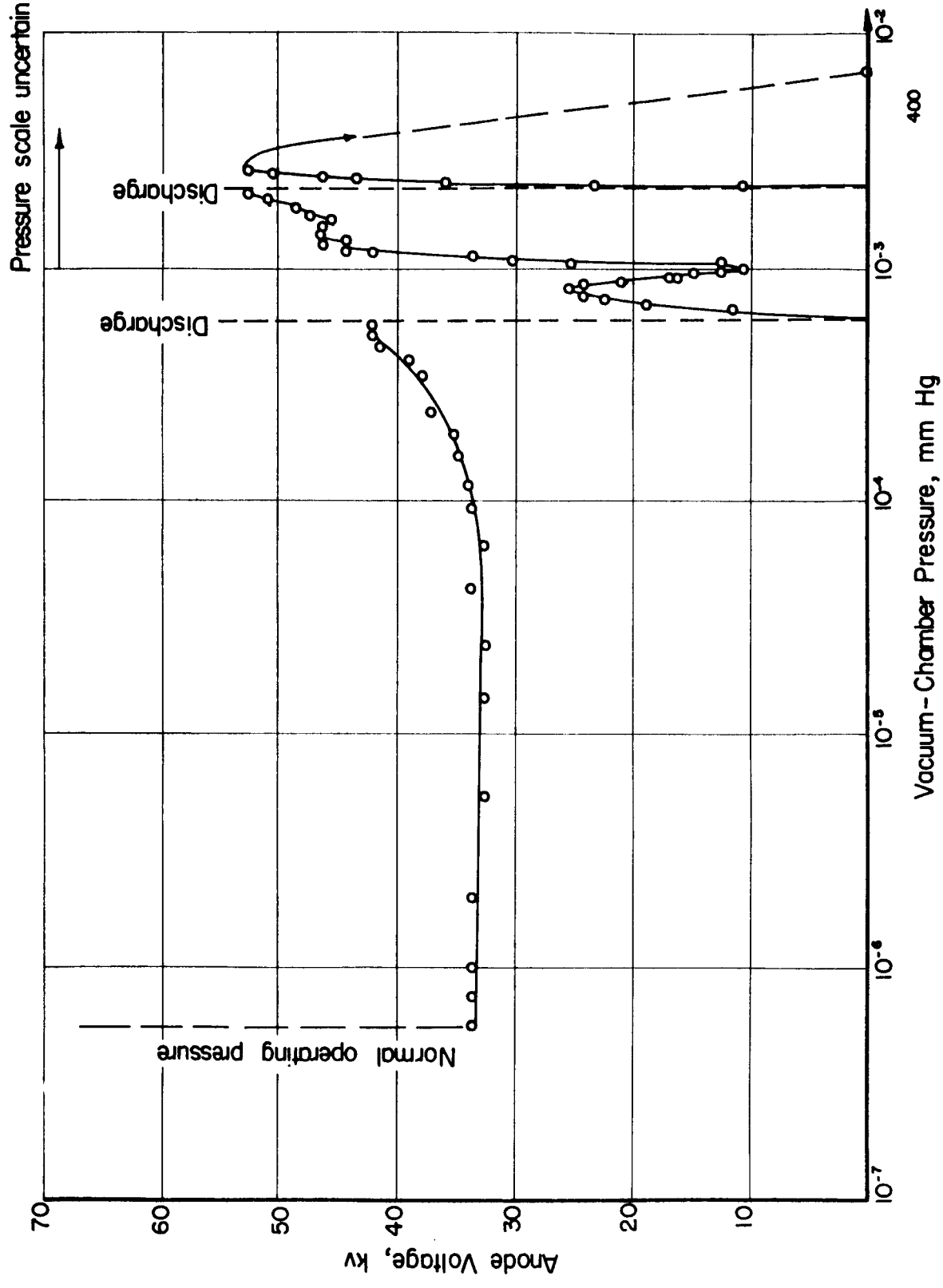

FIGURE 12. ALPHA CELL ANODE VOLTAGE VERSUS PRESSURE

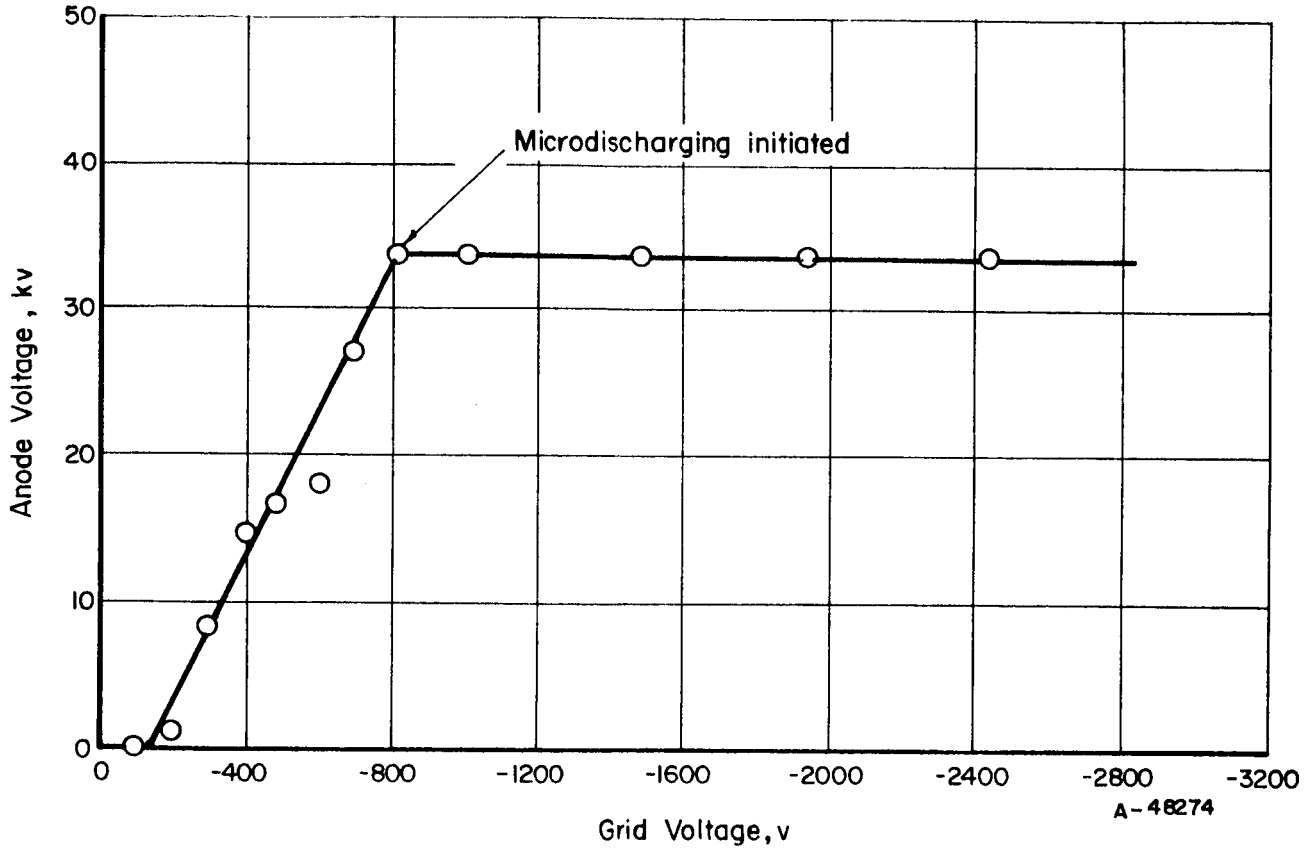

FIGURE 13. ANODE VOLTAGE VERSUS GRID BIAS

breakdown.[15] Interchange of current between electrodes at values below the critical current occurs in the form of microdischarges. It has been suggested[16] that the microdischarges are due to particles or clumps of foreign material ejected from the electrode surfaces by the electric field. Whatever the mechanism, simultaneous observations of microdischarges with voltage buildup with betas indicated that the discharges first occur at about 50 kv and then occur with increasing frequency up to a limiting voltage of approximately 100 kv. Presumably, at this voltage, the leakage current contained in the microdischarges offsets the charging current. The discharge frequency as a function of anode voltage is shown in Figure 14 for an experiment using the alpha-cell apparatus but using beta emission for voltage buildup. From very crude measurements, it has been estimated that about 10^{10} electrons are contained in each microdischarge. In the initial alpha-cell experiment, the voltage never exceeded the threshold voltage for onset of microdischarging of about 50 kilovolts. The appearance of the very definite threshold voltage for microdischarging explains the sudden stop in voltage buildup with time in the initial experiments.

Summary of Battelle-Sponsored Alpha Cell Experiments

The initial experiments gave a voltage buildup of about 50,000 volts, which was very encouraging. This was sufficient to prove the principle of operation (at least in the low voltage range) and to permit extraction of preliminary values of design parameters. The experiments also vividly showed the microdischarge problem to be the main experimental obstacle to obtaining higher voltages. The big question remaining at the conclusion of the initial experiments was that of how basic a limitation the microdischarging presented. The seriousness of this problem arises from the fact that the alpha cell is inherently a low-current device.

The next logical step in the demonstration of alpha cell feasibility appeared to be to extend the voltage capability to near the 1-megavolt range, where efficient operation is possible, and to determine the characteristics of the cell under these conditions. The problem of microdischarging would be attacked through insulator design, utilizing the presently available technology. The remainder of this section of the report describes the "second generation" of experiments performed under contract with NASA with apparatus redesigned to attempt high voltage buildup.

RESULTS OF EXPERIMENTS PERFORMED UNDER NASA CONTRACT

Experimental Apparatus

The equipment for the current alpha-cell experiment was redesigned on the basis of the earlier experience. The principal changes in the vacuum facility were designed to ease the loading and removal problems with the alpha emitter and to provide for a better support arrangement of the grid-cathode and anode assemblies. The principal changes in the design of the alpha-cell experiment itself were centered around the microdischarging problem and involved an increase of spacing between the cell components and a new type of insulator for the anode.

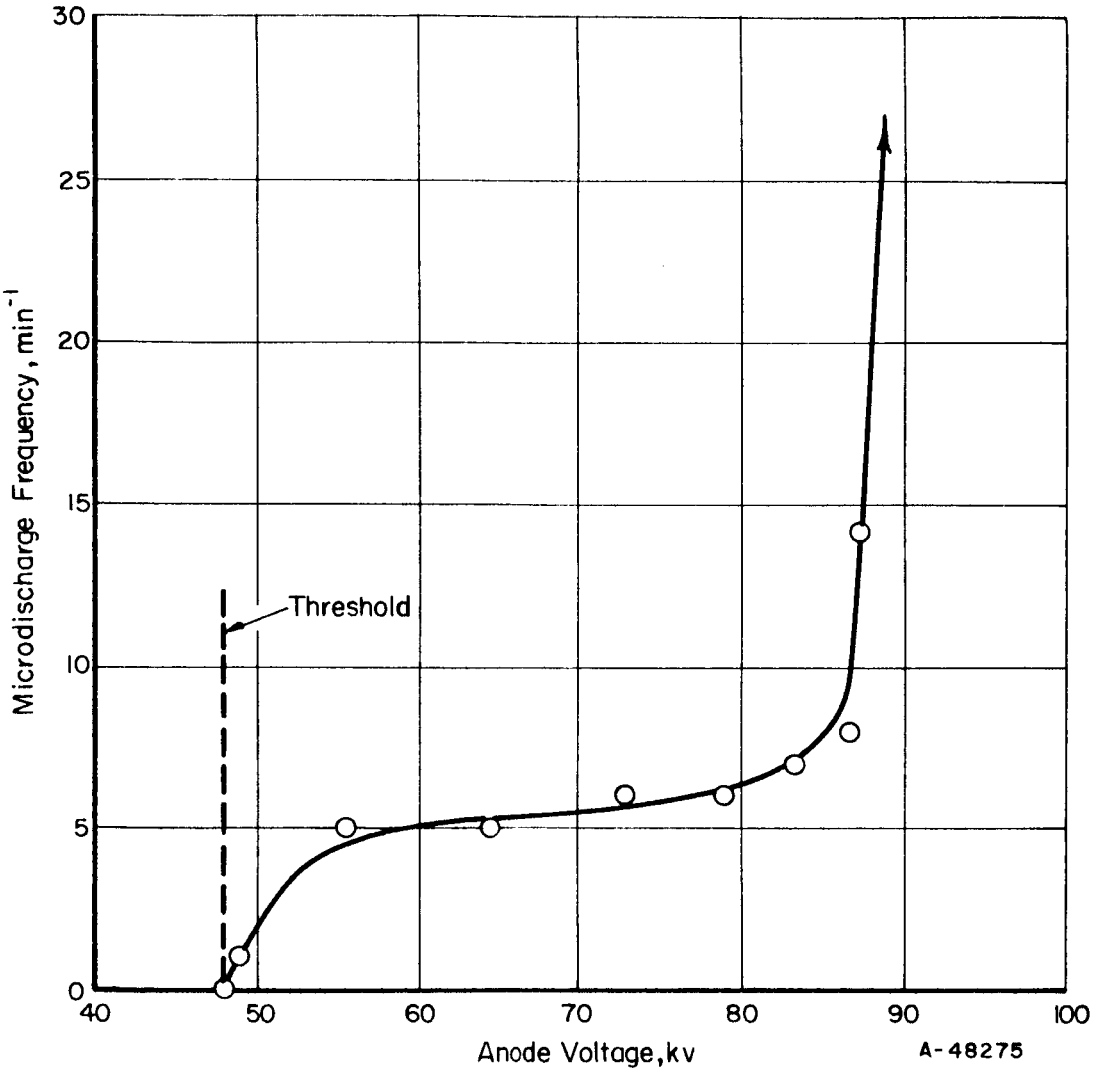

FIGURE 14. FREQUENCY OF MICRODISCHARGES VERSUS ANODE VOLTAGE

Vacuum-Facility Description

The high-vacuum system was designed to maintain a vacuum of 10^{-7} torr, a pressure shown by the initial experiments to be several orders of magnitude below that required to sustain 50,000 volts. Figure 15 is a photograph of the vacuum tank, showing the feedthroughs for the electrical connections and for the alpha voltmeter. The vacuum chamber is a 3/16-inch-thick Type 304 stainless steel bell jar 24 inches in diameter and 62 inches in height. As seen from the photograph the chamber is horizontally sectioned and flanged at approximately its midplane, providing unrestricted admittance for insertion of the experiment. Viewing ports on both halves of the chamber provide visual access to the experiment.

A 6-inch oil-diffusion pump having a maximum unbaffled pumping speed of 1440 liters/sec at 10^{-3} torr, backed by a 26-cfm mechanical compound pump maintains the vacuum at 10^{-6} to 10^{-7} torr without bakeout. An optically dense cold trap (Freon cooled) located immediately above the diffusion pump minimizes the back streaming of pumping fluid vapors. A 6-inch line with pneumatic valve connects the pumping complex with the vacuum chamber. The pneumatic valve in the 6-inch line together with a 2-inch pneumatic valve in the foreline protects the pumps and alpha-cell experiment against gross oil migration in the event of pump failure. Because of possible air-borne contamination from the alpha emitter, the exhaust vapor from the forepump exits into a leaktight exhaust stack through a Cambridge absolute filter. A cold trap in the exhaust line condenses oil vapors to prevent saturation of the absolute filter.

To expedite experiments determining the dependency of the cell currents and voltage on pressure, the vacuum chamber is equipped with a "variable leak". Conductance of the leakage is variable from 100 cm^3/sec to 10^{-10} cm^3/sec. Dry air is admitted to the chamber through the leak by passing room air through a 24-inch column of desiccant.

Alpha-Cell Experiment Design and Description

This section of the report describes the four principal components of the experiment: anode, cathode, grid and anode insulator. Figure 16 is a sketch of the alpha cell components installed in the vacuum facility which shows the arrangement of the various components.

Anode Design. The anode and anode-insulator assembly are shown in the photograph of Figure 17. The anode consists of a 6-inch-diameter aluminum tube which is highly polished, as seen from the photograph (average depth of surface irregularities estimated to be 1 to 10 microinches). The length of the straight portion of the anode is approximately 22 inches. At the bottom, the anode joins smoothly to a spherical dome which is supported by the anode insulator. The top end of the anode is open to receive the grid-cathode assembly. A lip arrangement is fitted onto the top end of the anode to reduce the electric field at the edges. The circular depression shown in the side of the anode is the holder for the small auxiliary alpha source used for the alpha voltmeter.

Insulator Design. Because of the microdischarging problem encountered in the Battelle sponsored experiments, particular emphasis was placed on insulator design. The quartz tripod arrangement used in the earlier experiments was abandoned,

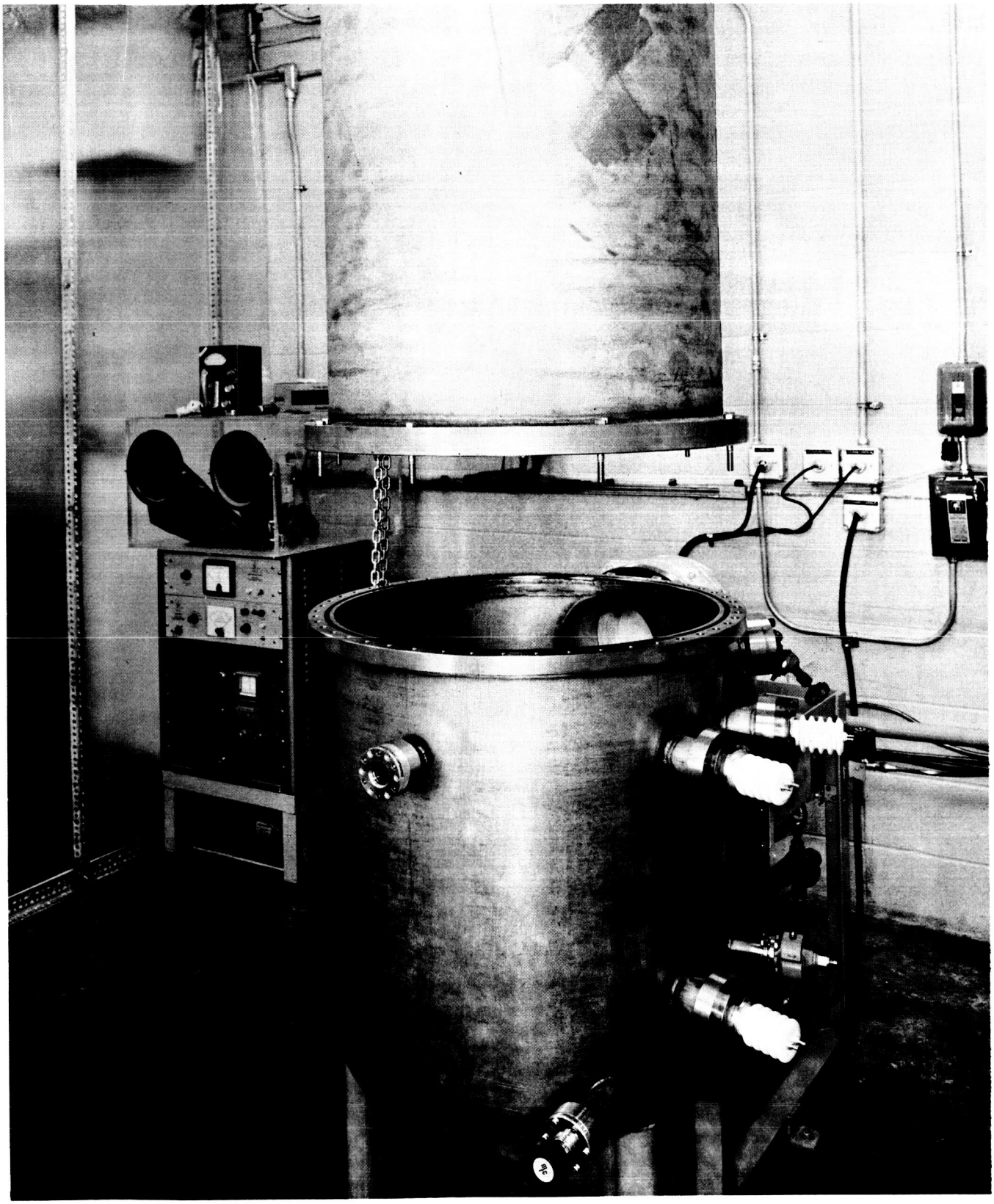

10491

FIGURE 15. VACUUM FACILITY FOR ALPHA-CELL EXPERIMENT

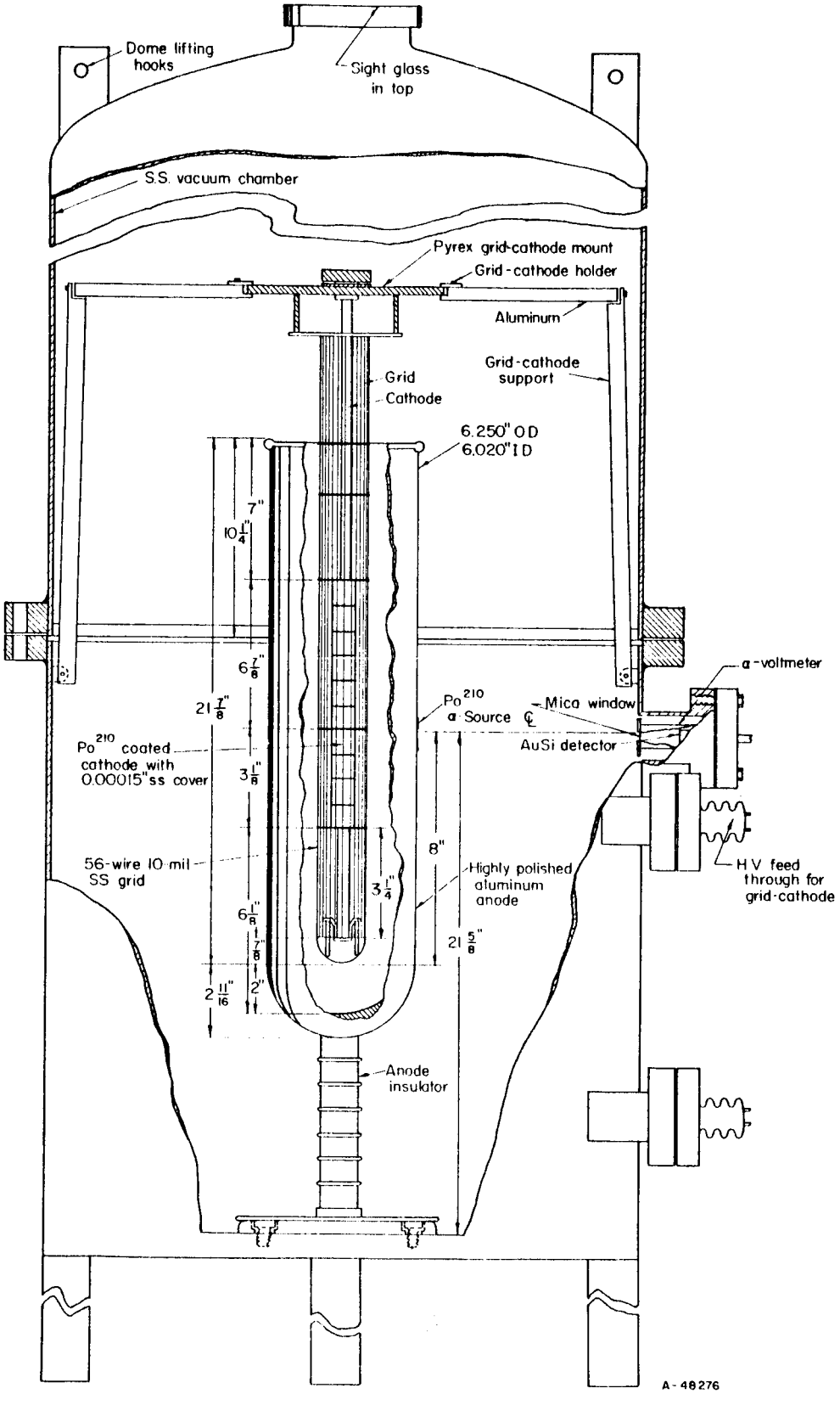

FIGURE 16. SKETCH OF ALPHA CELL EXPERIMENT ARRANGEMENT

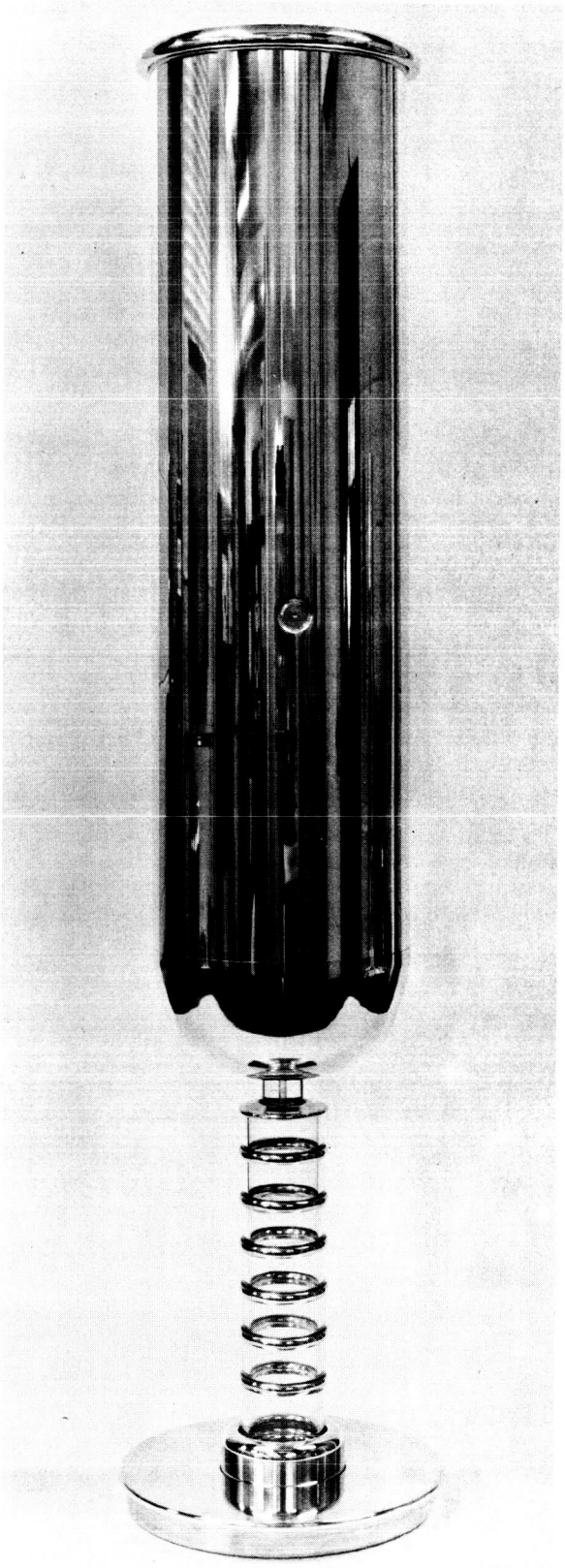

FIGURE 17. ANODE AND ANODE-INSULATION ASSEMBLY

10418

principally for structural reasons, in favor of a simple cylindrical geometry, shown in Figure 17 and sketched in detail in Figure 18. Pertinent information was gleaned from the literature to serve as a guide in insulator design. The principal observations and design reasoning are stated below.

(1) In the use of high-voltage insulators in vacuum, electrons and negative ions are preferentially emitted at, or in the immediate vicinity of, the negative junction. These gain energy in traversing the evacuated space toward the positive electrode and upon striking solid material liberate X-rays, secondary electrons, and ions. These secondary particles further the voltage-breakdown process. By recessing the insulator into the base making the negative junction, the breakdown voltage can be significantly increased.[17, 18]

Referring to Figure 17, the metal-to-dielectric junction, at the bottom of the insulator, was constructed with an undercut recess in the aluminum base. The insulating glass was attached with an epoxy resin. This recessing of the insulator combined with the use of epoxy resin reduces the high fields between the insulator and aluminum base.

(2) Although it has been observed that surface resistivity and certain other factors affect vacuum-breakdown voltages, each of these factors alone generally has a less striking effect than the junction phenomenon.[17] Since the insulator resistance must be greater than 10^{14} ohms, the readily available candidate materials are the glazed ceramics and hard glasses. Since both of these materials have similar surface resistivity, this parameter was not a factor in insulator design.

(3) The voltage at which electrons are released at the negative junction and the breakdown voltage both appear to be lower for materials of higher dielectric constant.[18, 19] Since hard glasses generally have lower dielectric constant, quartz was selected over a glazed ceramic as the insulator material.

(4) Voltage grading provides a uniform electric field along the insulator, thereby preventing a localized accumulation of charge and consequent flashover.[20]

The design of the anode insulator as a series of quartz rings separated by aluminum rings was based on the results of experiments performed at the Ion Physics Corporation.[20] The glass was bonded to the aluminum with epoxy. The available data indicate that each ring should be capable of sustaining about a 60-kv potential difference; the total stack therefore should support 400 to 500 kv. It should be noted that these design factors apply strictly only to the case of true high-voltage breakdown where currents are available of sufficient magnitude to cause flashover. It is assumed that these factors also apply in at least a general way to the micro-discharge problem where the total current available is of the order of 10^{-8} amp.

Cathode Design. The principal changes in cathode design over that used in the earlier experiments were an increase in the diameter of the emitting layer from 1/2 in. to 1.0 in. (to reduce the local electric field) and in the use of a covering of stainless

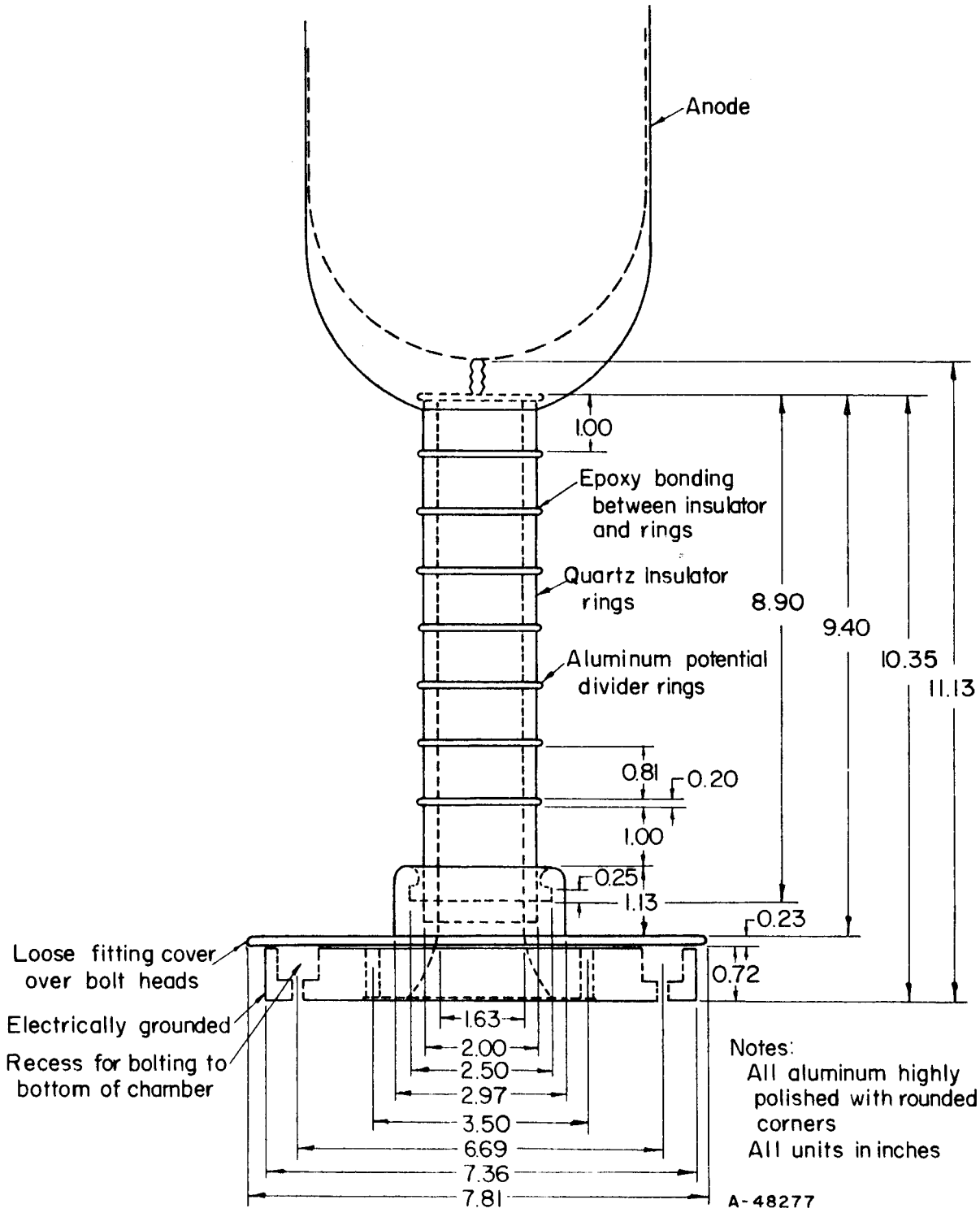

FIGURE 18. ANODE-INSULATOR DESIGN DETAILS

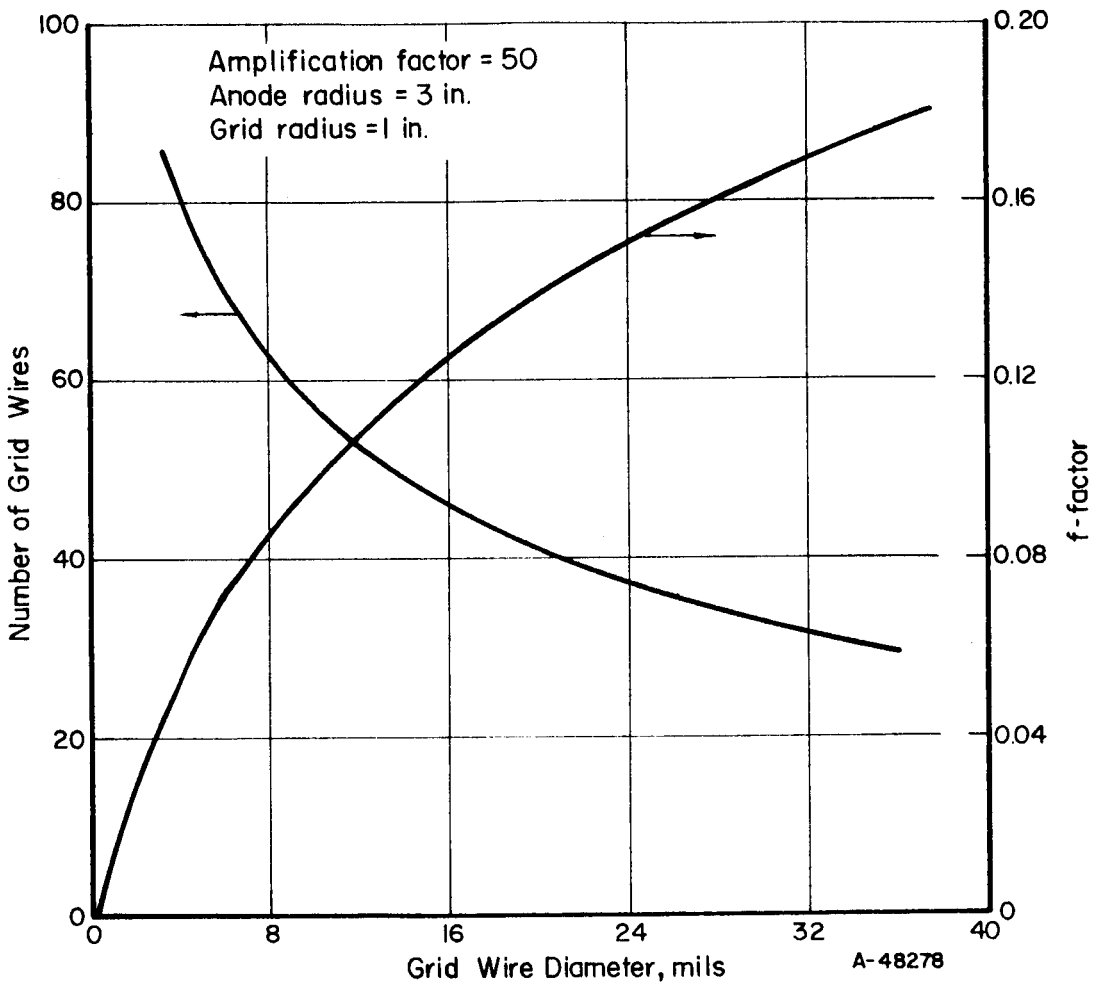

FIGURE 19. GRID DESIGN PARAMETERS VERSUS GRID WIRE DIAMETER

steel foil rather than gold. This latter change was made in an attempt to reduce gross contamination of the experimental apparatus due to migration of the alpha emitter. Polonium-210 was again selected as the alpha emitter for the purposes of the experiment because of its high specific activity (short half-life). The cathode was fabricated by the Monsanto Research Corporation.

The fueled portion of the cathode is 10 in. long and consists of three copper cylinders, each 3-1/3 in. by 1-in. OD. The copper was flashed with a thin coating of gold and then plated with a total of 8.85 curies of polonium-210 (June 4, 1964). Source strength at the time of the experiment was approximately 6 curies. Variation of the polonium content between the three cylinders was determined to be less than about 2 per cent. The source material was wrapped with a 0.00015-in.-thick stainless steel foil which extends the entire length of the cylinders. The end-point energy of the alpha particles leaving the foil is approximately 3.5 Mev, and the resolution of the energy-spectrum peak is between 10 and 15 per cent.

Grid Design. Grid design was based on the first-order principles stated previously in the discussion of the theory of operation of the alpha cell. With the dimensions of the cathode and anode given by other considerations, e.g., vacuum-facility dimensions, voltage breakdown, and end losses, the objective of the grid design was to achieve an amplification factor of 50 and an f-factor (screening fraction) of 0.1 or less. The amplification factor of 50 was based on the anticipated ability of the grid insulation to maintain a potential of 10 kv and on the anode insulator to support 500 kv. With given values for the grid-circle radius (1 in.), cathode radius (1/2 in.), and anode radius (3 in.), from Equations (26) and (28), the product (Nd_g) is determined, where N is the number of grid wires and d_g is the diameter of the wires. The results are shown in Figure 19, which gives the f-factor and number of grid wires required versus wire diameter to achieved the desired amplification factor with the given dimensions. As the graph shows, to obtain an f-factor of less than 0.1, the grid-wire diameter must be less than 11 mils. Selecting a 10-mil diameter to coincide with commercially available wire, the number of wires selected was 56, which is the even number closest to that indicated by the analysis. Using these values, the calculated f-factor and amplification factor of the grid are 0.0955 and 48.5, respectively.

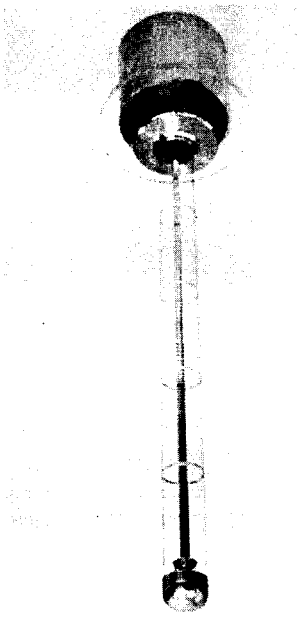

FIGURE 20. GRID USED IN ALPHA-CELL EXPERIMENTS

Figure 21 is a photograph of the alpha cell experiment installed in the vacuum chamber.

Instrumentation

The alpha cell is instrumented for measuring anode voltage, grid and cathode currents, and chamber pressure.

Anode voltage is measured using the previously described alpha-particle voltmeter. Figure 22 is a block diagram of the complete measuring circuit. The alpha particles emerging from the small anode source are detected through an air-filled chamber by a surface-barrier detector in conjunction with a charge-sensitive preamplifier and low-noise amplifier. The signal is then fed into a single-channel differential analyzer. With the analyzer in the differential mode (calibration channel), the signal is fed into a scaler-timer unit for determination of the range of the alpha particles in the small air-filled chamber in front of the detector. In the integral mode of operation (recording channel), the signal is directed to a ratemeter and then to a recorder for a direct anode-voltage reading.

Grid voltage is supplied by a 0 to 10-kv battery power supply. The grid and cathode currents are measured through Keithley Model 410 micromicroammeters. These currents can also be recording directly to study transient effects.

Pressure in the small alpha-voltmeter air chamber is determined from a mercury manometer. Pressure in the high-vacuum chamber is measured by a Hughes cold-cathode gage and control unit.

Preliminary Measurements and Calibrations

Prior to installing the polonium-coated cathode, system capacitances, insulator resistance and background currents were measured, and the alpha voltmeter calibrated. These results are briefly summarized below.

Capacitance and Resistance Measurements

The coefficients of capacitance and inductance for the four-electrode arrangement of the alpha-cell experiment (cathode-1, grid-2, anode-3, vacuum chamber wall-4) were determined from capacitance-bridge measurements. These measurements were corrected to obtain a charge balance on the system. The resulting matrix of coefficients, in units of micromicrofarads, is

$$(C) = \begin{pmatrix} 102 & -48 & -16 & -38 \\ -48 & 137 & -44 & -45 \\ -16 & -44 & 126 & -66 \\ -38 & -45 & -66 & 149 \end{pmatrix} , \qquad (44)$$

where the indices for the various electrodes are given above. The most important coefficient is $C_{33} = 126\ \mu\mu f$, the capacitance of the anode to ground.

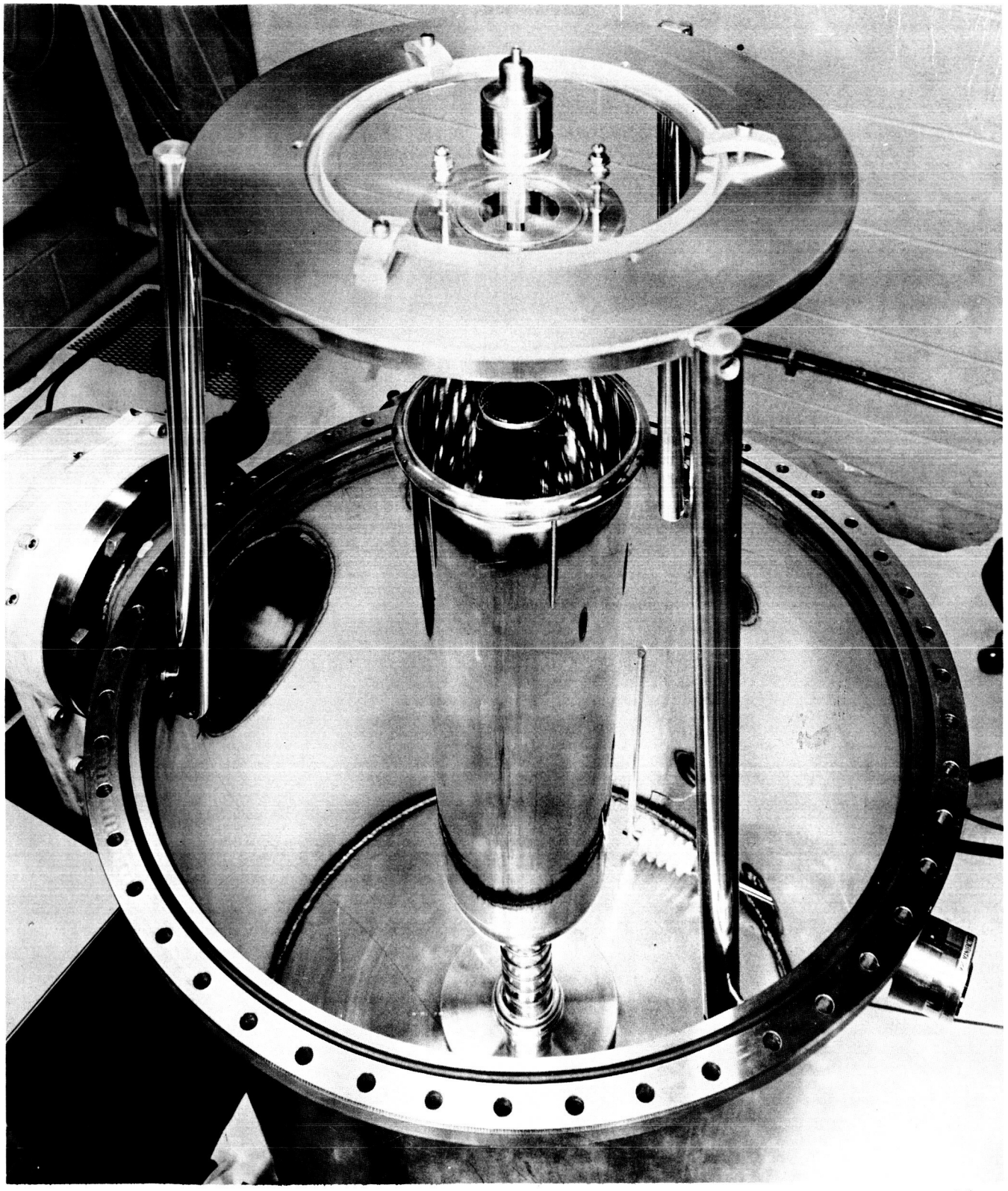

12670

FIGURE 21. ALPHA-CELL EXPERIMENT INSTALLED IN VACUUM CHAMBER

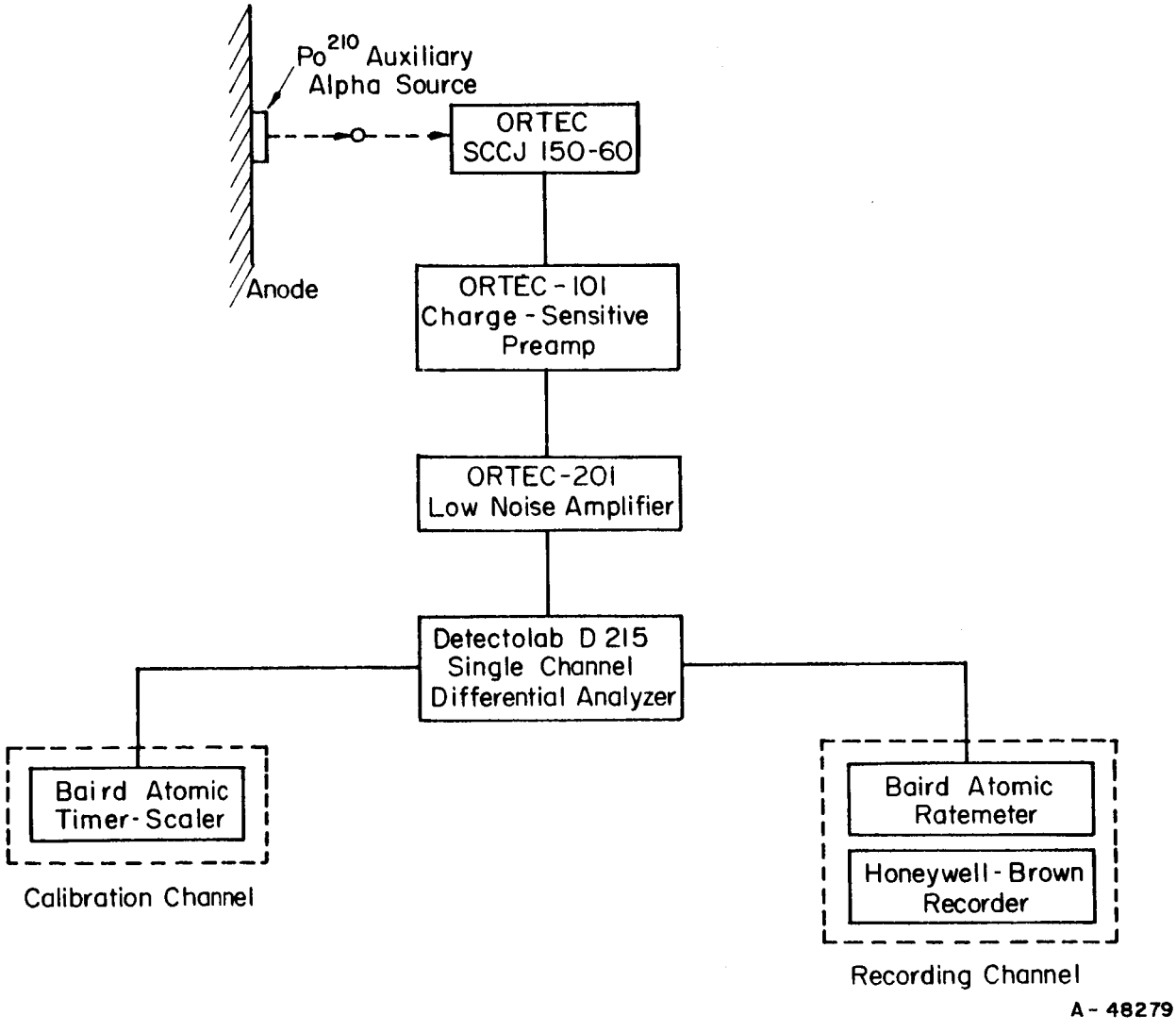

FIGURE 22. ALPHA-VOLTMETER CIRCUITRY

Because of the extremely high resistance of the anode insulator, the magnitude of its resistance could not be determined. However, time-constant determinations showed its value to be much greater than 10^{14} ohms, which is sufficiently large to produce a negligible drain on the anode during operation of the experiment.

Grid and Cathode Currents With No Alpha Emitter

The grid and cathode currents were determined to be of the order of 10^{-11} amp with no alpha emitter on the cathode. As will be seen from later data, these currents are several orders of magnitude below the currents present with the fueled cathode (10^{-8} to 10^{-7} amp), and thus no correction to the fueled data is required for background currents. The principal source of the small residual grid current is leakage in the battery power supply.

Alpha-Voltmeter Calibration

As mentioned previously, the alpha voltmeter operates on the principle of change of alpha-particle range in air with alpha-particle energy. Figure 23 shows the total (integral) count rate detected by the surface-barrier detector as a function of air pressure in the thin-windowed chamber interposed between the detector and a small (23 millicuries) polonium-210 source mounted on the anode (at the position shown in Figure 17). The lower curve is the base-line curve obtained with the anode grounded. Although this voltage-measurement technique is rather inaccurate below about 50 kilovolts, a check on the voltmeter performance was obtained by applying 30 kilovolts to the anode from an external power supply and observing the shift in the count-rate curve. These data were then compared with the predicted shift based on the alpha particle range-energy relationship. The results, shown in Figure 23, indicate excellent agreement.

For a fixed pressure, the range of linearity of voltage with count rate is limited. The nonlinearity can be accounted for by measuring the shift in energy spectrum of the alpha particles striking the surface-barrier detector. (This method, in fact, can be used over the entire range of interest but is experimentally inconvenient.) The peak shift is determined by a multichannel analyzer substituted in the calibration channel of the alpha-voltmeter circuit (see Figure 22). The channel shift was calibrated in terms of energy change by determining the channels at which the peaks of known alpha emitters occurred. For this calibration, plutonium-239 (5.14 Mev) and polonium-210 (5.30 Mev) bare, thin sources were used, with typical results as shown in Figure 24. Also shown in this figure is the zero-voltage energy spectrum of the alpha particles seen by the surface-barrier detector through the mica window of the voltmeter chamber. Assuming linearity of the channels with energy, the polonium-210 and plutonium-239 calibrations both yield 0.0248 Mev/channel. A rough check on the assumption of linearity was made by comparing the channel shift between the two calibration sources. This comparison yields 0.027 Mev/channel, with at least 15 per cent error, which is in good agreement with the linear value of 0.0248 Mev/channel.

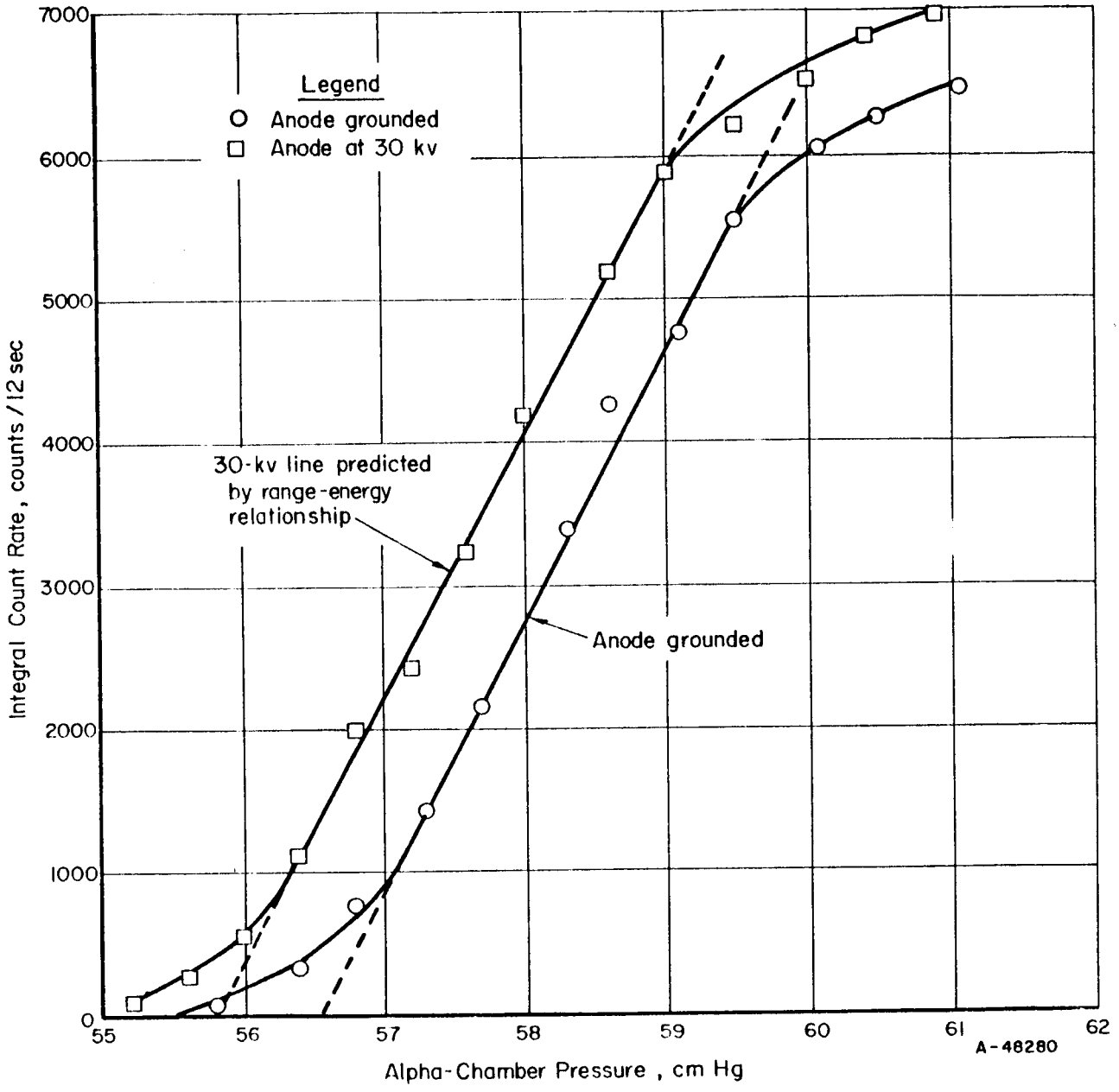

FIGURE 23. LOW-VOLTAGE INTEGRAL COUNT RATE VERSUS PRESSURE FOR ALPHA VOLTMETER

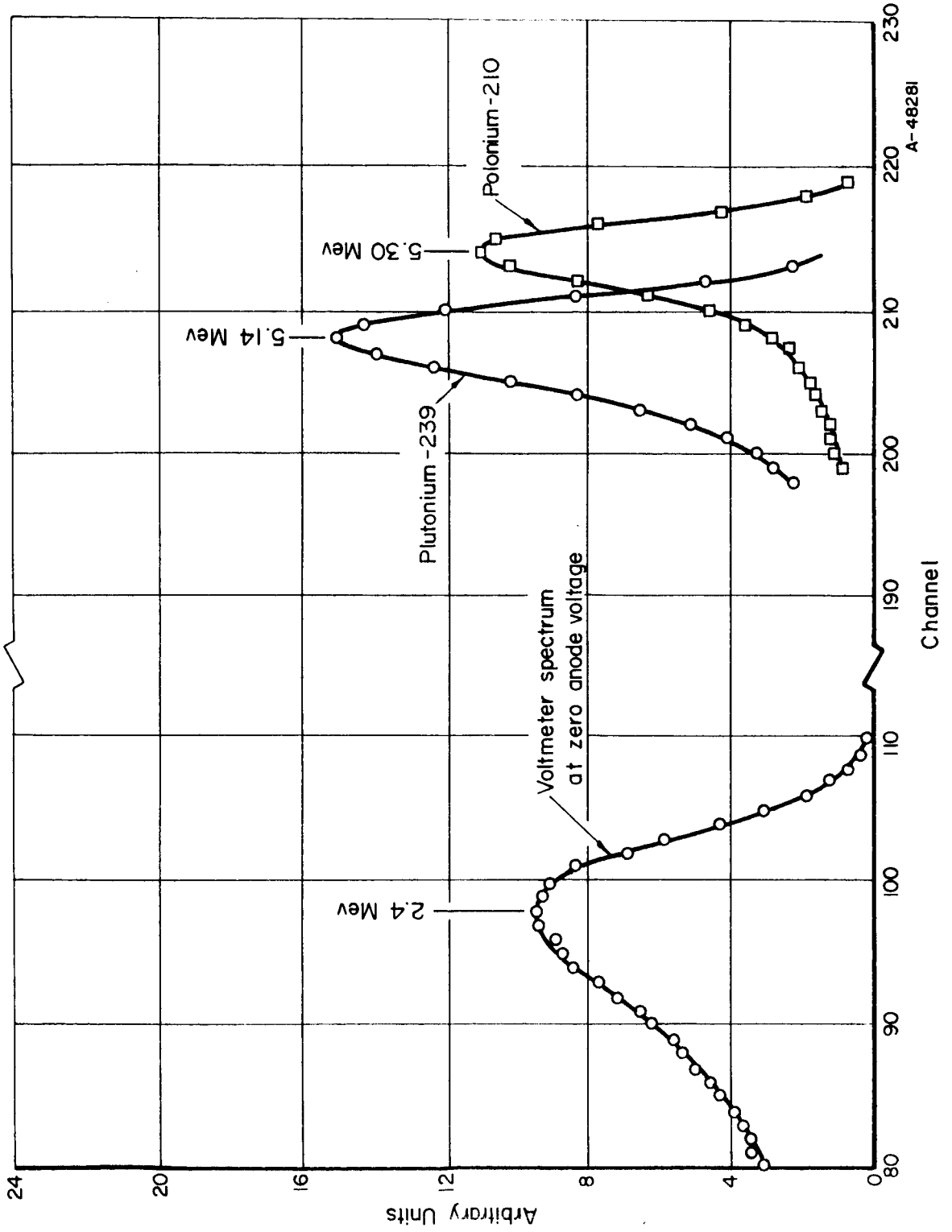

FIGURE 24. ENERGY SPECTRUM OF VOLTMETER ALPHAS AND ENERGY CALIBRATION OF ANALYZER

Initial Experiments With the New Alpha Cell

Upon completion of the measurements and calibrations with no alpha emitter present in the experiment, the polonium-coated cathode described previously was inserted into the vacuum chamber and initial data obtained from the new experiment. The results are presented below with a minimum of analyses; further data accumulation and analyses of the results are currently in progress.

Cell Currents With Anode Grounded

The first important result required from the experiment is to demonstrate that a net positive current flows upon application of negative voltage to the grid. To obtain this information, the cathode current I_{co} and grid current I_g were measured as a function of negative grid bias with the anode grounded. These data are shown in Figure 25. The results show that the net current I_c from the grid-cathode assembly, which is the algebraic sum of the grid and cathode currents, is indeed positive; thus voltage buildup can be expected when the anode is ungrounded. Comparison of these data with the results of earlier experiments (Figure 9) shows that the behavior is similar in the two cases. There is a small current exchange between grid and cathode in the new cell, shown by the non-zero slopes on these curves, but the net current appears to be independent of grid bias at large voltage. Other differences in the currents between the two experiments are due to differences in polonium source strength and in grid design. The magnitude of the net charging current (1×10^{-8} amp) is consistent with estimates based on the known source strength and estimated current losses due to the presence of the grid.

Detailed current-voltage behavior in the range of 0 to ±300 volts was also obtained for analysis of the secondary-electron-emission parameters. In general these data are consistent with the results of earlier experiments and indicate a secondary-electron yield of approximately 10 electrons per alpha particle emerging from the cathode.

Initial Voltage Buildup

The approach to high-voltage operation was initiated with the new emitter installed. This approach will involve a series of steps with appropriate data at each voltage level. The first level, 100,000 volts, was successfully achieved just prior to this publication and is a factor of two higher than that achieved in earlier experiments. This voltage level was accurately predicted from the calculated amplification factor for the grid of 48.5 when using present grid bias of -2000 volts.

Detailed performance data are now being collected at this 100-kv level to provide input for the analyses. Further increases in voltage will be sought by application of larger grid biases. Microdischarging was observed at 100 kv and may again limit voltage buildup at some higher voltage.

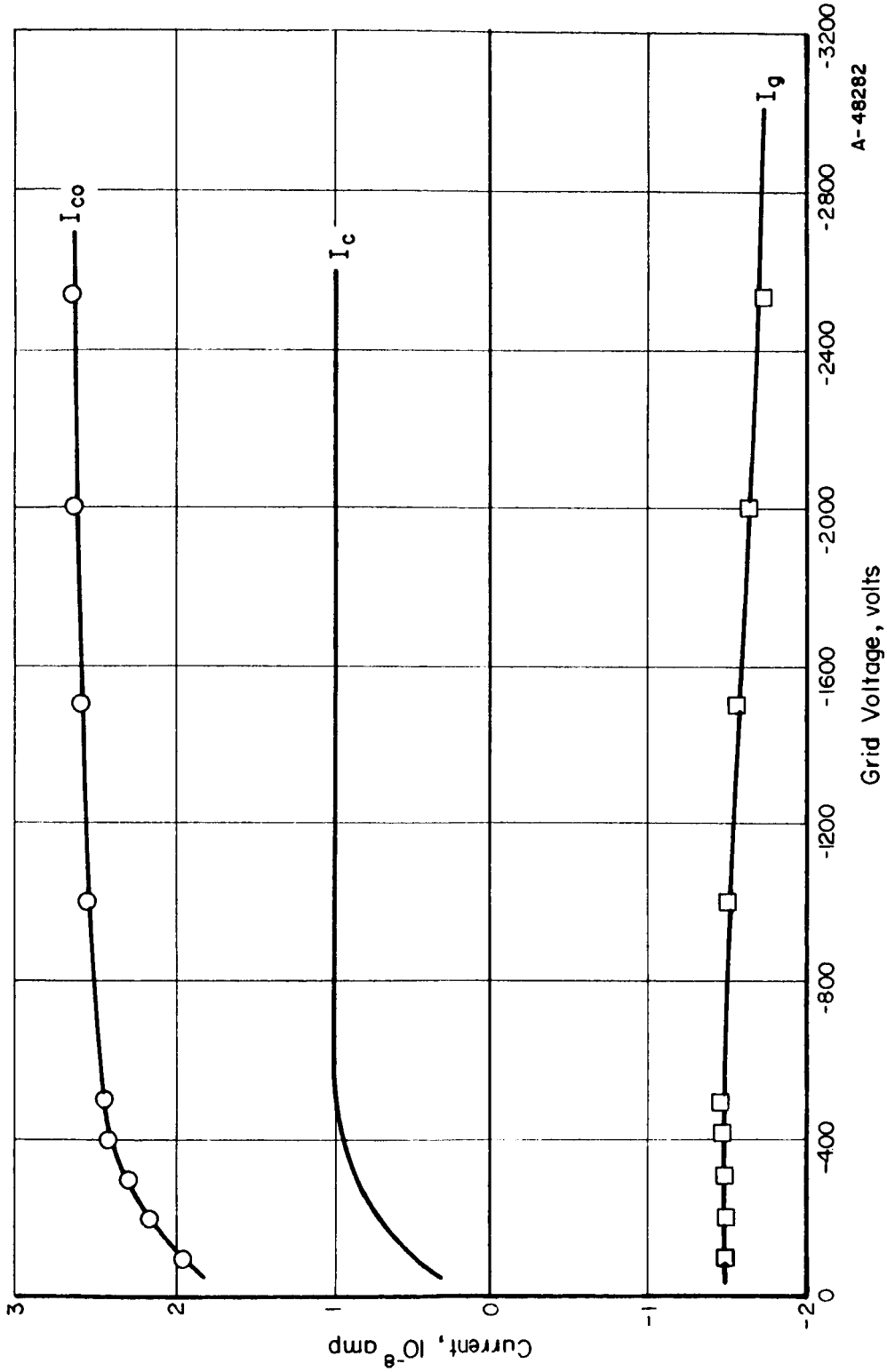

FIGURE 25. CELL CURRENTS VERSUS GRID VOLTAGE WITH ANODE GROUNDED

INVESTIGATION OF METHOD OF ELECTRICAL-POWER CONVERSION

Although the principal objective of this program is to determine the behavior of the alpha cell in the megavolt range of operation, a concurrent investigation is being conducted to evaluate techniques to transform cell output from the megavolt to the kilovolt range. The goal is to produce a conceptual design of a conversion system which will provide the required voltage transformation with minimum power loss. The design of such a system depends to a large extent on the cell characteristics which are yet to be determined, but several conversion concepts have been investigated in a general manner to determine the approach best suited to the somewhat unusual characteristics of the alpha cell.

Two general approaches to a conversion scheme have been taken. One of these (ballistic method) involves the production of an oscillating or pulsating output by means of forces applied to the charged particles within the cell, while the other involves the production of a pulsating voltage by means of external circuits to which the cell output is applied. Because of the requirement that the alpha cell must operate at a high voltage level to maintain peak efficiency, the ideal converter is one which produces the desired output voltage and waveform without causing a large shift in the operating voltage of the cell.

Power Conversion by Particle-Ballistic Methods

In general, particle ballistic methods of power conversion do not appear to be promising. The problems encountered with this approach are illustrated by the examples given below.

One of the concepts considered, which approaches the ideal converter from the standpoint of not changing the operating voltage, is shown in Figure 26. The scheme here is to replace the grid wires with radial fins and to replace the solid anode with a segmented electrode. An alternating output would be produced by focusing the alpha particles alternately on two sets of anode segments. In the figure, the "A" segments would be connected electrically and isolated from the "B" segments, which would likewise be electrically connected. The alpha particles would be focused alternately on the two sets of anode segments by applying different voltages alternately to adjacent grid fins. The applied grid voltage would always be negative, however, to suppress secondary-electron emission at the cathode. Although this scheme appears to meet the requirements of an acceptable converter, an investigation of the particle ballistic shows that because of the high deflection voltage required it is not feasible to assemble a cell with necessary fin spacing to prevent electrical breakdown between adjacent fins. An alternative means of producing the desired particle deflection is with a magnetic field. The required field strength is reasonable, but because of the relatively large volume through which the field must be applied, this scheme is not considered a practicable one at this time.

Another alpha-particle ballistic method considered to produce an alternating output applies the klystron concept to a beam of particles directed out of the cell. It appears that beam focusing can be accomplished by using the anode for electrostatic focusing. However, this method is not being given further attention because of the relatively large drift space required (tens of meters).

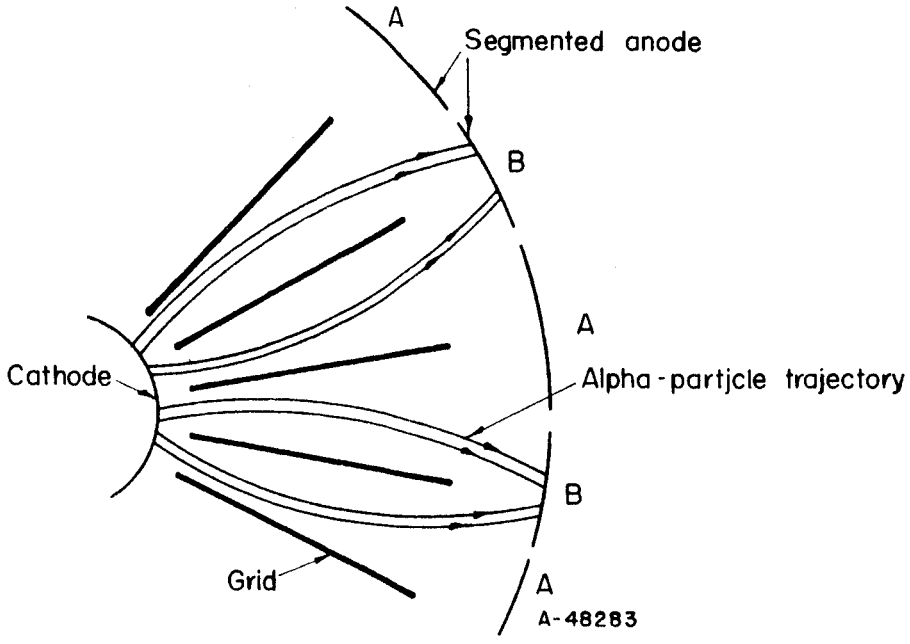

FIGURE 26. BUNCHING OF ALPHA PARTICLES BY MEANS OF A FINNED GRID

The possibility of producing an alternating output by causing the cell to oscillate by means of a feedback circuit has also been investigated. While this scheme is possible, it has the disadvantage that the average power output is considerably less than the maximum capability of the cell because of the low operating efficiency at low output voltage.

Power Conversion by External Circuitry

Two methods have been considered for converting the cell output to a lower voltage by means of external circuits. The first of these involves the series charging and parallel discharging of a bank of capacitors. One possible arrangement is shown in Figure 27. In this circuit, the triggering of a high-voltage gap is followed by the breakdown of low-voltage gaps, thus causing the entire capacitor bank to discharge in parallel through the load. For a bank of N capacitors, the output voltage is 1/N times the cell output voltage, and the total charge available at the load is N times that of each capacitor. In practice, the low-voltage gaps would be such that complete discharging would not occur so that cell operating voltage could be maintained in the region of high efficiency. Two problems which require further consideration are the high-voltage gap, which must withstand the full cell output voltage, and the physical size of and power losses in the inductors. A similar scheme, employing resistive rather than inductive elements, has been suggested but has been given only secondary consideration because of the complicated switching required to produce the parallel and series configuration.

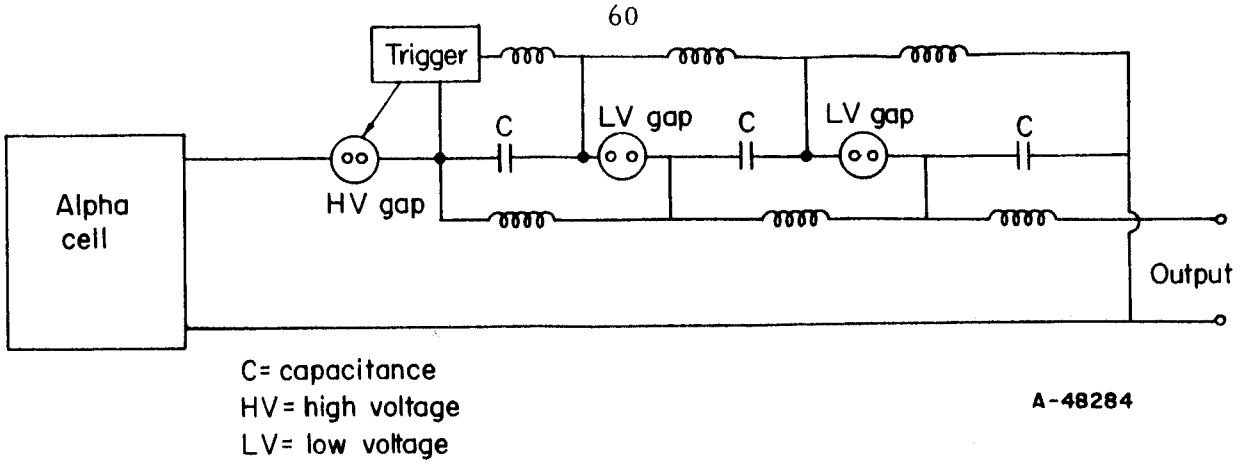

FIGURE 27. SERIES CHARGE-PARALLEL DISCHARGE CONVERTER

The concept that appears most promising at present is an external conversion circuit employing piezoelectric transducers. The interesting feature of this technique is that the transducers themselves are high-voltage insulators and can be incorporated in the physical design of the cell. The converter would consist of a number of piezoelectric elements in series across the high-voltage output of the cell. This high-voltage assembly would be mechanically coupled to an assembly of parallel-connected elements. High voltage applied to the series assembly would produce a physical expansion which would apply a force to the parallel-connected assembly through a mechanical linkage, thereby inducing an output voltage. The output-voltage level is determined by choice of piezoelectric material and size of the transducers. The equivalent circuit for this electromechanical transformer is shown in Figure 28. Two problems are now recognized as possible limiting factors in the application of this transformer to the alpha cell. First, the physical size of the primary (high-voltage) side of the transformer may be larger than desirable (of the order of a meter for one of the commercially available transducers) and, second, with a d-c cell output it is necessary to bleed off the charge accumulated in the primary side to provide for continued operation, thus introducing undesirable power losses. However, because the scheme appears to be well-suited to this application and is inherently efficient, it is being investigated further.

SUMMARY OF WORK PERFORMED DURING FIRST HALF OF PROGRAM

The work performed on Contract No. NAS3-2797 during the first 4 months is briefly summarized below:

(A) Experimental Studies

(1) Constructed, installed and put into operation the apparatus for alpha-cell experiments

(2) Performed preliminary measurements and calibration prior to installing alpha emitter

(3) Performed initial measurements on alpha cell with anode grounded to obtain basic parameters for analysis

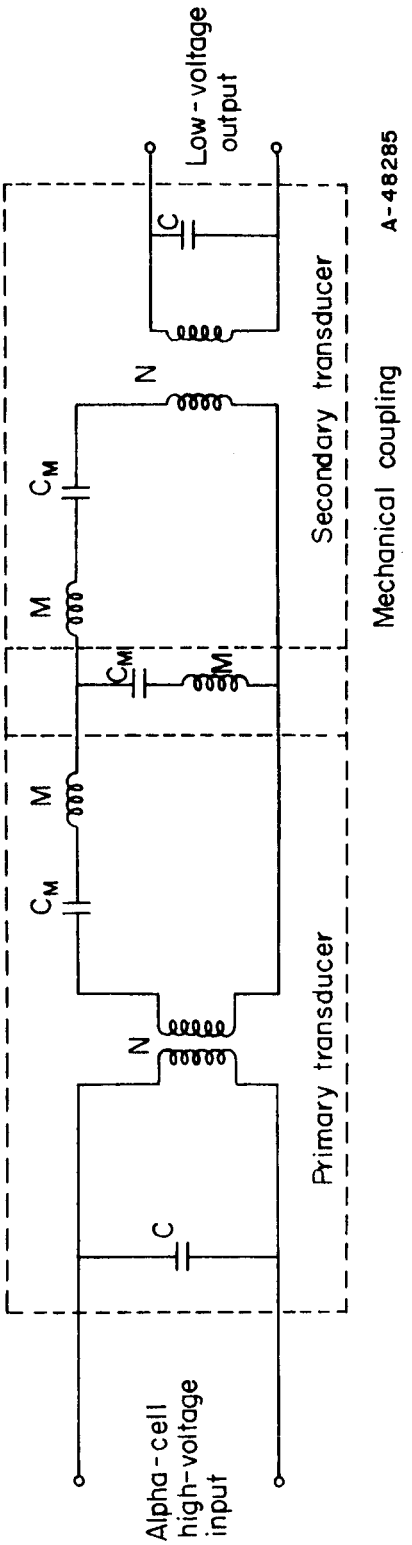

FIGURE 28. ELECTROMECHANICAL-TRANSFORMER EQUIVALENT CIRCUIT

(4) Performed primary voltage-buildup experiments.

(B) Analytical Studies

(1) Performed analysis in support of experiment design and construction

(2) Performed analyses on data from preliminary measurements and calibrations

(3) Analyzed effect of "fall-back" alpha particles on cell currents and efficiencies

(4) Performed preliminary investigation of power-conversion techniques for the alpha cell generator.

SUMMARY OF FUTURE PLANS

During the second half of the program, the following studies are planned.

(A) Experimental Studies

(1) Continue stepwise approach to higher cell voltage, taking appropriate data at each attained voltage

(2) Determine current-voltage behavior of new cell under various conditions

(3) Determine effect of grid voltage on anode voltage (amplification factor)

(4) Determine sensitivity of cell currents and voltage to cell pressure

(5) Observe transient responses of cell currents and voltage to grid-voltage variation.

(B) Analytical Studies

(1) Conclude analysis of experimental data on current-voltage behavior to evaluate critical parameters that enter into theoretical predictions of cell efficiency and performance

(2) Analyze grid control on anode voltage

(3) Analyze the effects of the changes made in the new cell design on cell performance

(4) Evaluate degradation of alpha-particle energy spectrum with emitter coating thickness

(5) Conclude investigation of power-conversion techniques and produce a conceptual design of a conversion system

(6) Outline development program required to provide operational alpha cell devices.

It should be mentioned that several of the analytical studies planned for the second half of the program have already been initiated but are in early stages. The bulk of the analytical work is related to Item (1).

REFERENCES

(1) H. G. J. Mosely, and John Harling, "The Attainment of High Potentials by the Use of Radium", Proc. Roy. Soc., 88, 471-476 (1913).

(2) E. G. Linder, and S. M. Christian, "The Use of Radioactive Material for the Generation of High Voltage", J. Appl. Phys., 23, (11), 1213-1216 (November, 1952).

(3) J. N. Anno, "Secondary Electron Production From Alpha Particles Emerging From Gold", J. Appl. Phys., 34 (12), 3495-3499 (December, 1963).

(4) Karl R. Spangenberg, Vacuum Tubes, First Edition, McGraw-Hill Book Company, Inc. (1948), p 128.

(5) Karl R. Spangenberg, op. cit., p 137.

(6) L. Cranberg, J. Appl. Phys., 23, 518 (1952).

(7) J. R. Greening, "Contribution to the Theory of Ionization Chamber Measurements at Low Pressure", British Journal of Radiology, 27, 167 (March, 1954).

(8) Unpublished data by J. N. Anno, Battelle Memorial Institute.

(9) Alfred Schock, "A Direct Nuclear Electrogenerator", ASTIA, AD 216 712 (June 15, 1959).

(10) Harold L. Davis, "Radionuclide Power for Space – Part I", Nucleonics, 21, 61 (March, 1963).

(11) H. Geiger, Handbuch der Physik, Vol 24, edited by S. Flugge, Springer-Verlag, Berlin (1927), p 171.

(12) J. W. Kennedy, et al., "Some Experiments on Electrical Conduction in Vacuum", AECU-3989.

(13) L. H. Bettenhausen and W. J. Gallagher, "An Alpha-Particle Voltmeter", Nucleonics (June, 1964).

(14) Bethe, Rev. Mod. Phys., 22, 217 (1950).

(15) A. Maitland, J. Appl. Phys., 32 (November, 1961).

(16) N. I. Ionov, "Mechanism for Prebreakdown Conductivity in Vacuum Interelectrode Gaps", Translated from Zhurnal Tekhnicheskoi Fiziki, 30 (5), 561-567 (May, 1960).

(17) M. J. Kofoid, "Effect of Metal-Dielectric Junction on High-Voltage Breakdown Over Insulators in Vacuum", AIEE Transactions, 999-1004 (December, 1960).

(18) M. J. Kofoid, "Phenomena at the Metal-Dielectric Junctions of High-Voltage Insulators in Vacuum and Magnetic Field", AIEE Transactions, 991-999 (December, 1960).

(19) P. H. Gleichauf, "Electric Breakdown Over Insulators in High Vacuum", J. Appl. Phys., 22 (5), 535-541 (1951).

(20) R. B. Britton, K. W. Arnold, and A. S. Denholm, "Ability of a Voltage-Graded Surface to Support a High Voltage in Vacuum and in a Pressurized Gas", Rev. Sci. Instr., 34, 185-187 (February, 1963).

BIBLIOGRAPHY

(1) J. N. Anno, "A Direct-Energy-Conversion Device Using Alpha Particles", Nuclear News, Vol. 5, No. 12, 3-6 (December, 1962).

(2) A. M. Plummer and J. N. Anno, "Battelle Studies on the Triode Concept of Direct Energy Conversion", a paper presented at the Summer Institute on Direct Conversion at the University of Illinois, July, 1963.

(3) A. M. Plummer and J. N. Anno, "Conversion of Alpha Particle Kinetic Energy Into Electricity", ANL-6802, pp. 170-180, AMU-ANL Conference on Direct Energy Conversion, November 4-5, 1963.

AMP:WJG:RGM:JNA/so